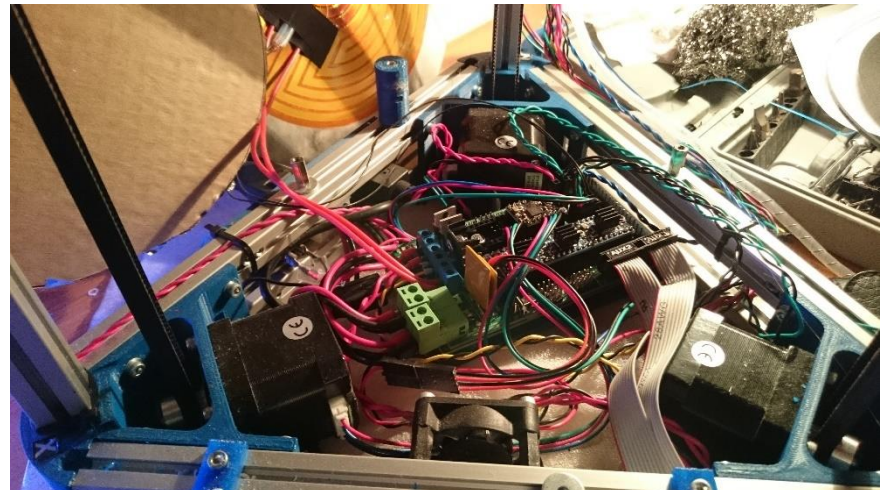
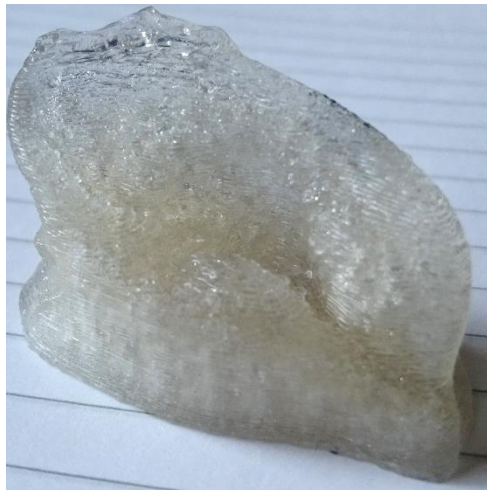
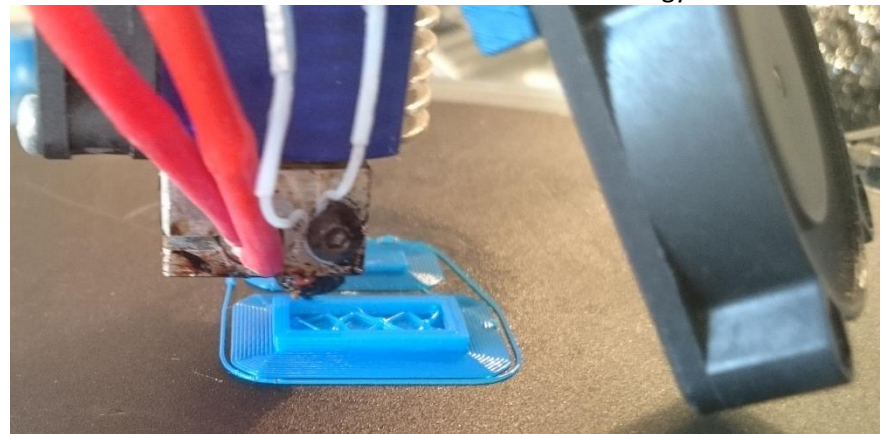


Fabian Trauzettel



Cork Institute of Technology



# 3D Printing soft PVC – Final Report

Fabian Trauzettel – R00086027

Supervisor: Michael Walsh

BEng(Hons) Biomedical Engineering – Cork Institute of Technology

May 2016

# Contents

Abstract.....	5
Acknowledgements.....	5
Introduction .....	6
Literature Review.....	7
CAD/CAM and the Digital toolchain.....	8
Effect of a shortened toolchain on Research and Development.....	8
3D printing processes.....	9
1. Photopolymerisation (also called SLA, or Stereolithography) .....	9
1. Binder jet.....	10
1. Fused deposition modelling (FDM).....	11
Patent Search .....	12
Assessment of Process suitability .....	13
1. Photopolymerisation.....	13
2. Binder jet.....	14
3. Fused deposition modelling.....	14
CNC technology.....	14
Control of motors.....	14
Programming.....	14
Types of FDM printers.....	15
1. Cartesian .....	15
2. Delta.....	15
Theory of PVC plasticisation .....	17
DEHP (Bis(2-Ethylhexyl) Phthalate).....	17
Ethical Issues .....	18
Project Management .....	19
First Semester .....	19
Second Semester.....	20
Initial Testing.....	21
Purpose of testing:.....	21
Apparatus:.....	21
Experimental Setup.....	21
Extruder.....	22
Temperature Control .....	23
Circuitry.....	25
Procedure.....	27
Example calculation .....	27
Results.....	28

Temperature datalogs.....	29
Discussion.....	30
Systematic Design .....	31
List of primary objectives.....	31
Possible solutions.....	33
Metrics .....	35
Metrics tables.....	35
Design choice .....	36
Peristaltic Pump Design .....	37
Calculations.....	37
Testing of initial design .....	39
Peristaltic pump redesign .....	39
Gearbox design .....	40
Pump calculations for redesigned pump .....	42
Theoretical steps per mm of “filament” .....	43
Installation of modified hot end .....	45
Discussion of first feed system test .....	46
Corrective actions taken in response to results from feed system testing .....	48
1. Nozzle clog problem.....	48
2. Replacement of the peristaltic pump .....	48
3. Bubble reduction / degassing .....	49
Calibration of new pump .....	49
PVC 3D printing .....	52
Degassing system controller design.....	53
Comparison of 3D printed PVC with conventionally manufactured PVC .....	55
ISO 37:2011 – Rubber, vulcanised or thermoplastic – determination of tensile stress-strain properties .....	55
Dumbbell test pieces.....	55
Tensile testing .....	59
Procedure.....	59
Tensile testing results, 3D printed .....	60
Tensile testing results, Cast.....	61
Discussion of tensile testing results.....	62
Conclusion.....	62
References .....	63
 Figure 1 - SLA process .....	9
Figure 2 - binder jet process .....	10
Figure 3 - FDM process .....	11

Figure 4 [14] viscosity profiles of plastiols at different temperatures. The dioctyl phthalate profile is of particular interest.....	13
Figure 5 - Cartesian 3D printer.....	15
Figure 6 - RepRap Mendelmax 3.0.....	15
Figure 7 - Delta-type 3D printer .....	16
Figure 8 - The RepRap Kossel Mini used for this project .....	16
Figure 9 - the conventional hot end in the process of disassembly. Note the disconnected carbon fibre rod on the left. ....	16
Figure 10 - Semester 1 Project Schedule .....	19
Figure 11 - Semester 1 Gantt Chart .....	19
Figure 12 - time plan for first and second semester.....	20
Figure 13 - Bench Testing.....	21
Figure 14 - Extruder test rig .....	22
Figure 15 - e3d v6 hotend.....	22
Figure 16 - Steinhart-Hart model of Semitec 104GT2 thermistor .....	25
Figure 17 - schematic of temperature control circuit.....	25
Figure 18 - circuit on prototyping board.....	26
Figure 19 - Graph of Temperature vs corrected mean pressure .....	28
Figure 20 - temperature profile, climbing to 210°C.....	29
Figure 21 - temperature profile, climbing to 200°C.....	29
Figure 22 - Syringe driver .....	33
Figure 23 - peristaltic pump .....	33
Figure 24 - progressive cavity pump .....	34
Figure 25 - gear pump .....	34
Figure 26 - lobe pump .....	34
Figure 27 - first iteration of peristaltic pump.....	38
Figure 28 - 3D printed prototype, assembled with tubing and NEMA 17 stepper motor .....	38
Figure 29 - A4988 stepper motor driver connection diagram .....	39
Figure 30 - epicyclic gearing .....	40
Figure 31 - redesigned peristaltic pump .....	41
Figure 32 - Planetary gear mechanism, printed in blue PLA.....	44
Figure 33 - Peristaltic pump with planet/bearing carrier installed.....	44
Figure 34 - Peristaltic pump, fully assembled .....	44
Figure 35 - upgraded DRV 8825 stepper driver (top left, purple PCB) installed on printer motherboard .....	44
Figure 36 - lid of peristaltic pump with tubing installed .....	44
Figure 37 - modified effector plate .....	45
Figure 38 - effector plate installed in printer, and all electronics connected. note the hose barb visible in the center of the effector .....	45
Figure 39 - extrusion test with peristaltic pump in background.....	46
Figure 40 - extruded PVC showing air bubbles .....	46
Figure 41 - degraded PVC plug .....	47
Figure 42 - purchased peristaltic pump .....	48
Figure 43 Pololu A4988 stepper motor driver connected to Arduino .....	49
Figure 44 - simple water calibration setup .....	50
Figure 45 - 3D printed PVC puck .....	52
Figure 46 - scaled-down model of a human ear, printed in soft PVC .....	52
Figure 47 - Schematic of Arduino-based vacuum controller .....	54
Figure 48 - Vacuum pump controller PCB .....	55
Figure 49 - ISO 37 type 4 dumbbell. All dimensions in mm.....	56
Figure 50 - mould for production of cast test pieces.....	56
Figure 51 - filling a mould with PVC .....	57

Figure 52 - Dumbbell mould in the oven to cure.....	57
Figure 53 - 3D printer producing a PVC object .....	58
Figure 54 - Cast and 3D printed tensile testing samples side-by-side .....	58
Figure 55 - cast test piece in tensile tester jaws .....	59
Figure 56 - Stress-Strain curve, 3D printed PVC.....	60
Figure 57 - Stress-Strain Curve, Cast PVC.....	61

## Abstract

The goal of this project was to develop a process with which to 3D print using soft PVC. To this end, first semester was spent determining the feasibility of designing a 3D printing system for a soft PVC material. A patent and internet search showed that no methodology for this process has been developed as of the time of writing. Research, experimentation and design work was carried out to evaluate the material's suitability for printing by a Fused Deposition Modelling process. Experiments carried out showed that the process is indeed feasible using off the shelf components and at pressures attainable at sufficiently small scales to be implemented in an FDM-type desktop 3D printer. In second semester, issues were encountered such as a redesign of the feed system pump, under extrusion, clogging and bubble formation. Solutions for these issues were found and implemented. With these problems solved, it was possible to 3D print some basic diagnostic pieces as well as a large demo piece in the shape of a scaled-down human ear. Tensile tests according to ISO 37 were carried out to determine the various material characteristics of the 3D printed PVC. Results were compared to results obtained for cast PVC samples. Initial results suggest that the 3D printed PVC may have an ultimate tensile strength about 43% higher than the same material does when cast, however more research is needed before conclusions can be drawn.

## Acknowledgements

I would like to thank:

Michael Walsh, for his aid in finding a suitable space to conduct experiments and guidance regarding the project;

Sean F O'Leary for his encouragement to go ahead with my proposal;

Paddy Collins for his help sourcing power supplies for my experiments;

John McDonald at Teleflex medical for his support of my project and for his mentorship;

Roland Maichel, Laboratory manager at Willy Rüsch GmbH, for his advice and sharing his wealth of experience with me;

And Thomas Palm, Engineer at Willy Rüsch GmbH, for his encyclopaedic knowledge of PVC.

## Introduction

There is currently no method for the production of prototypes made of soft PVC using additive manufacturing, despite the ubiquity of the material. Soft PVC is used extraordinarily widely; in everything from slush-moulded soft toys to textured coatings and medical devices. It would therefore be beneficial to the state of the art to develop a rapid prototyping process that utilises this common material.

While PVC has been increasingly criticised in the media due to the harmful effects of some plasticisers used to make the material soft and workable, it is still an outstanding material for the production of medical devices, as very few other polymers or elastomers achieve the same levels of simultaneous flexibility and biocompatibility as PVC.

This combination of mechanical and biological suitability has led to widespread adoption in the manufacture of tracheal tubes, catheters, as well as being a material for general tubing for IV's and fluid containers, including long-term blood contact device such as blood transfusion bags. In fact, PVC medical devices make up approximately 40% of all plastic medical devices in use today.<sup>[1]</sup> The material was originally used to replace more expensive devices manufactured from natural rubber, latex and glass and helped to usher in the age of cheap, disposable medical devices which are sterilised during manufacture.

Indeed, the material has been so successful in the medical industry that it has been in use for more than 50 years<sup>[2]</sup>. All uses included, Europe processes approximately 4.9 million tonnes of PVC per year, representing 11% of the plastics market in Europe in 2009<sup>[3]</sup>, making it the 3<sup>rd</sup> most commonly used plastic in Europe.

Currently, the medical industry uses several manufacturing processes for soft PVC, the two most widely used being extrusion and dip coating. Extrusion is used mainly to manufacture tubing and PVC sheeting to be used in the manufacture of blood bags or similar products, while dip coating can be used to manufacture parts such as tracheal tubes, which have a relatively large outer diameter and rely on geometry that is difficult to manufacture in any other way. Neither of these processes are capable of manufacturing parts with different geometry without major tool changes – for instance, if the diameter of a tracheal tube needs to be changed, the dipping rods themselves need to be replaced – this can be costly and time-consuming, making research and development of new products slow and difficult.

3D printing can circumvent this problem due to its ability to produce almost any imaginable geometry – this is achieved by constructing a model layer by layer, from the bottom up. As a result, even the most complex and radically different shape can be produced without modifying the machine itself, reducing the investment of time and resources required to produce prototypes.

## Literature Review

Polyvinyl Chloride (PVC) is the polymer form of Vinyl Chloride (also called chloroethene), which is produced from the combination of ethylene with chlorine in either suspension, emulsion, or mass polymerisation processes.

PVC was first discovered in 1872 by the German chemist Eugen Baumann. While Baumann was experimenting with Vinyl Bromide, a chemical closely related to Vinyl Chloride, he found that exposing the Vinyl Bromide to direct sunlight caused the formation of a solid, which he described as "white, or weakly yellow, sometimes opaque as porcelain, sometimes partially translucent as glass"<sup>[4]</sup>. This discovery led him to investigate whether the same reaction occurred with Vinyl Chloride. He prepared three tubes with anhydrous Vinyl Chloride. One tube was left anhydrous and placed in the dark. Another was mixed with a few drops of water and placed in direct sunlight; the third was also anhydrous and placed in direct sunlight. The latter two formed a white precipitate within 6-7 hours. After 8 days, the contents of both tubes had formed "bright white, completely opaque masses"<sup>[4]</sup>. These he described as "exceedingly tough, cohesive, non-crystalline, of a bright white colour and completely odourless".

He further analysed that the compound contained between 56.53% and 56.65% Chlorine - this is consistent with the chemical formula for PVC:



(PVC has a molecular mass of 61.49u, of which Chlorine makes up 57.65% with a mass of 35.453u)

The early 20th century saw attempts at large scale polymerisation of Vinyl Chloride. Initial efforts failed, due to general difficulties in working with the material; in 1912 Ivan Ivanovich Ostromislensky and Fritz Klatte separately attempted to industrialise manufacturing processes for PVC, with both filing patents. Ostromislensky failed in the face of high decomposition rates at the processing temperatures and Klatte only succeeded in producing a brittle PVC that degraded with exposure to elevated temperatures and light.<sup>[5]</sup>

In 1926 Waldo Semon, working for the BF Goodrich Company in the US, discovered that by mixing PVC with Tritolyl Phosphate and Vinyl Acetate the glass transition temperature could be lowered sufficiently to avoid the decomposition issues faced by Ostromislensky, while simultaneously mitigating the brittleness encountered by Klatte. These discoveries allowed PVC-P to become a huge commercial success, finding use in everything from building materials (PVC cladding or piping) to medical devices or food packaging (flexible medical tubing, airtight seals on glass jar lids).

While the tritolyl phosphate used by Semon is neurotoxic<sup>[6]</sup>, PVC-P manufactured using less harmful plasticisers is used for tubing, including medical tubing such as haemodialysis kits or IV lines, as well as other applications where flexibility and atraumatic properties are important, such as tracheal/tracheostomy tubes, or urinary catheters. In these use cases, plasticisers are used to modify the mechanical properties of the material by increasing its flexibility and changing its colour from an opaque white to a glassy transparent appearance.

## CAD/CAM and the Digital toolchain

Computer-aided design (CAD) and computer aided manufacturing (CAM) have become the mainstay of engineering design ever since computers have become powerful enough to render complex shapes in real time. The sequence of processes that lead from a CAD model to a physical object is known as the toolchain. In most cases, this toolchain will look something like this:



However, when designing and prototyping soft PVC components to be made using conventional processes, the toolchain becomes far longer, being extended past simple processes such as milling or turning, as the tooling for each part needs to be created before any parts can be made. This means that the toolchain in these cases begins to look more like this:



Needless to say, this is incredibly inefficient for the production of small-run components.

The toolchain for rapid prototyping is drastically shorter:



The fact that modern rapid prototyping machines can directly produce prototypes in a large variety of materials with totally different properties simultaneously and as a self-contained unit greatly amplifies this benefit. Furthermore, manufacturers of CAD software, such as Autodesk, are beginning to embrace rapid prototyping by directly including the ability to interface with slicing software through a dedicated environment within the CAD package. This environment allows the user to predetermine the scale, units, resolution and orientation of the stereo lithography file passed on to the slicer, saving time and increasing ease of use.

## Effect of a shortened toolchain on Research and Development

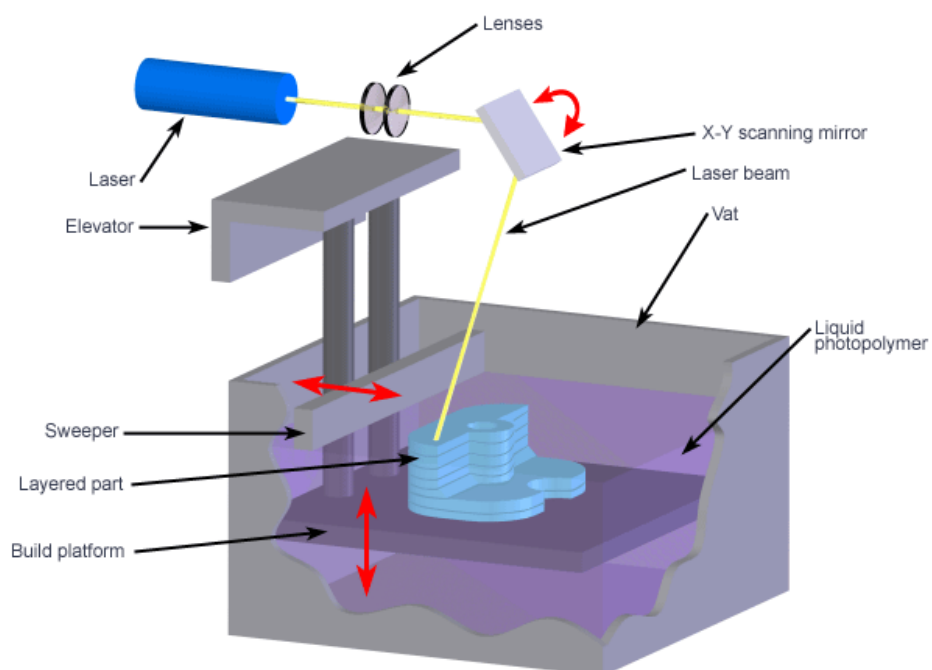
Financial consulting company Deloitte provides an interesting appraisal on the impact of 3D printing on Research and Development. While most companies approach the matter from the perspective of a reduction in cost for prototype production, Deloitte's analysis points out that it is the increased speed of prototype production that is the main benefit of the technology. According to the company, the increased speed and reduced cost per prototype will mainly lead to more design approaches being tried, improving outcomes and timelines, but not overall R&D costs. [7]

## 3D printing processes

A number of different 3D printing processes exist. A basic overview is given below:

### 1. Photopolymerisation (also called SLA, or Stereolithography)

In the photopolymerisation process, the printer consists of a vat of photopolymer resin which cures when exposed to ultraviolet light. Submerged in the resin lies a platform elevator, which holds the object to be printed. During printing, a laser in the ultraviolet spectrum traces out the shape of the part to be printed on the surface of the resin. This causes the resin to harden in the areas hit by the laser, forming one layer of the model. The elevator is lowered, and the next layer is traced out. A sweeper may be used to ensure there is adequate fresh polymer available. The process is pictured below:



Copyright © 2008 CustomPartNet

Figure 1 - SLA process

The process creates highly accurate models with very fine details – Stereolithography has been used to create parts with layer heights as small as 50µm, and features of 10µm can be faithfully reproduced. [8]

## 1. Binder jet

3D printers employing the binder jetting process use a liquid jet print head, much like a conventional inkjet printer, to precisely add binder to a powder. The printer itself holds a large container of powdered material. The bottom plate of the container can move vertically, to allow the layers to be built upward. The print head deposits binder in the required layer pattern, and a sweeper moves the next layer of powder into position, at which point the process is repeated. Once the print is complete, the finished part is retrieved from the container and cleaned of any remaining loose powder. Some more advanced machines can add ink to the binder, allowing the printer to produce multi-coloured parts.

### Inkjet: Binder Jetting

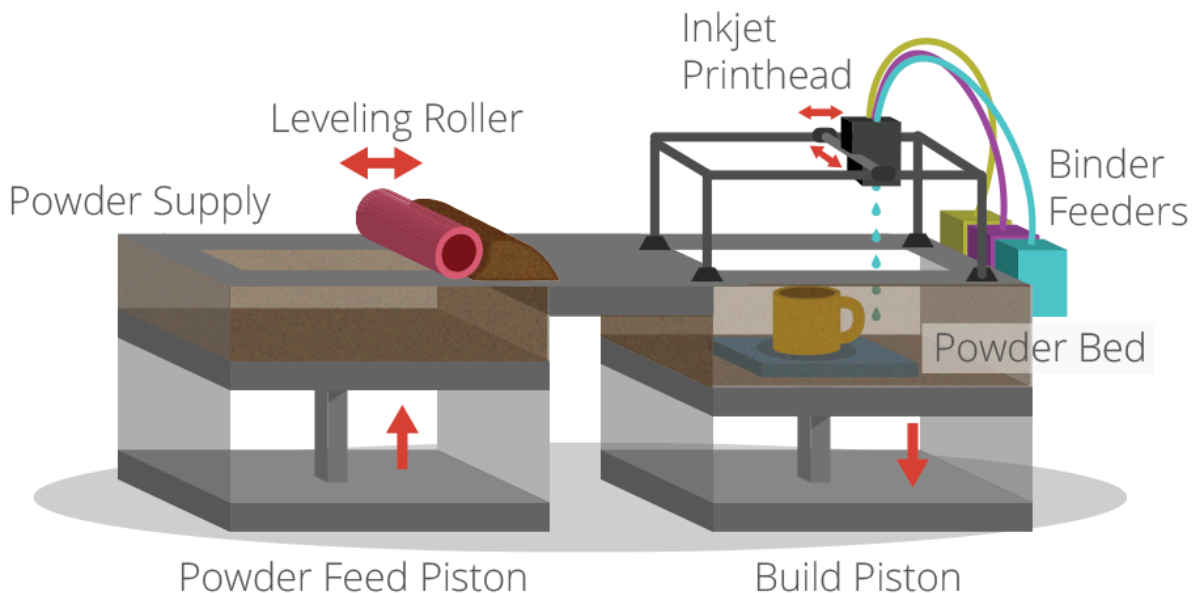


Figure 2 - binder jet process

Binder jet processes have become extremely versatile in recent years, with the entire field seeing massive investment into increasing the variety of materials available for printing. Most recently, Stratasys, one of the leading manufacturers of binder jet 3D printers, developed a range of flexible materials with hardness values in the Shore-A range (soft rubber hardness). Dubbed the “Tango” family of materials, they are available in a range of colours from translucent to greys and blacks. Furthermore, the powder-based process allows these elastomers to be combined with ABS-related powders, meaning that with just two materials, the printer can produce a range of 9 hardness values from shore 27 to 95 (a hardness range from softer than a pencil eraser to harder than a car tyre). [9]

### 1. Fused deposition modelling (FDM)

FDM 3D printers use a plastic filament and heated extruder to build up layers on a print bed. The filament is stored on a spool, and fed through to the nozzle by a set of rollers. The nozzle is then moved in the XY plane to trace out a layer. Once the layer is complete, the nozzle is lifted up in the Z direction, and the next layer is printed. The process is repeated until the model is complete. A 3D printer may or may not use a dual-nozzle system – one nozzle for the material, the other for support material. If support material is used, the supports are removed by dissolving them in a solvent bath which leaves the main material intact. This process is mostly used for ABS and PLA, however other materials such as nylon or wood or bronze-filled filaments can also be used.

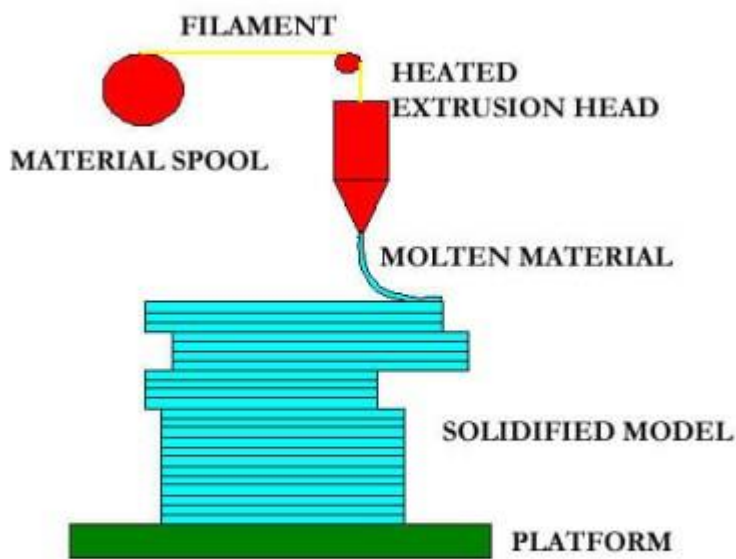


Figure 3 - FDM process

FDM printing is the methodology most favoured by the open-source 3D printing community due to the comparative ease with which FDM machines can be built; a large ecosystem of DIY 3D printers has developed since the original 20-year patent filed by S. Scott Crump in 1992<sup>[10]</sup> expired. Most famously, the RepRap project set up at the university of Bath, England has hugely influenced the spread of 3D printing by building FDM machines which build their own structural components, meaning that once one machine is built, others can be assembled more easily in a “pay-it-forward” style system. These FDM systems are somewhat limited in their resolution, typically limited to 0.1mm to 0.01mm features and tend to be comparatively unreliable, frequently needing recalibration and re-zeroing of their axes. However, these machines have proven sufficient for domestic users to print anything from trinkets and basic mechanisms to replacement parts for household items or specialised tools for DIY enthusiasts as well as prosthetics for children which “grow” with the child by simply printing new parts. The 2013 Wohlers report recorded an average annual growth of 346% in the area of personal 3D printers from 2008 to 2011. The majority of this growth has been attributed to the open-source rereprap project.<sup>[11]</sup>

## Patent Search

A 2013 report by the UK intellectual property office [12] shows that between the years 1980 and 2013 9145 patent publications were issued, across 4015 patent families. Unsurprisingly, the expiration of the FDM printing patent in 2012 caused year to show the peak number of patent applications in the time frame. The top patent-issuing organisation in the report is named as the USPTO, and accordingly, the US has been the top country for inventors applying for patents in the field.

In order to investigate prior work potentially associated with this project, a patent search was conducted on the websites of both the United States patent office as well as the European patent office. The following search terms were used:

- PVC plastisol additive manufacturing
- PVC plastisol 3D printing
- Plastisol 3D printing
- Plastisol additive manufacturing
- PVC 3D printing
- PVC additive manufacturing

The following results were obtained:

Search Term	USPTO	EPO
PVC plastisol additive manufacturing	0 Patents	2 Hits - none relevant
PVC plastisol 3D printing	0 Patents	0 Patents
Plastisol 3D printing	0 Patents	0 Patents
Plastisol additive manufacturing	0 Patents	0 Patents
PVC 3D printing	0 Patents	19 Hits - none relevant
PVC additive manufacturing	0 Patents	49 hits - none relevant

This does not, however, imply a clear field on the path to securing potential IP generated through the project. As the UK IPO report shows, Hundreds of patents are applied for annually in the field, and many of these patents simply exist to prevent a competitor from utilising a technology, rather than securing an IP owner's right to the sole use of the technology.

A better approach would be to make use of alternative licensing schemes such as the Creative Commons license. Developed in the US as an alternative copyright and IP protection system, CC licenses allow users to access and use the intellectual property for themselves, as long as the user does not adapt the licensed IP for commercial use. CC licenses have become enormously common in the open-source 3D printing world due to their relative ease of use (there is no registration required) and the fact that they allow easy and crowdsourced development of technology through internet forums. [13]

## Assessment of Process suitability

In order to assess the suitability of each of the above processes to the material, they must be analysed in terms of the chosen PVC compound. The PVC chosen for this project, P206, is a liquid in its raw state. The liquid is called a plastisol, a suspension of PVC particles in plasticiser (DEHP, Diethyl Hexyl Phthalate, also called dioctyl phthalate, DOP), epoxidised soybean oil, extender resin, copolymers and other additives. The viscosity of the raw material is approximately 100 mPaS at room temperature.

At temperatures approaching 50°C, PVC plastisols plasticised using DEHP begin to become more viscous, by a process called gelling. During this process, the PVC particles as well as the plasticiser begin to mutually dissolve each other, resulting in a steep increase of the suspension's viscosity.

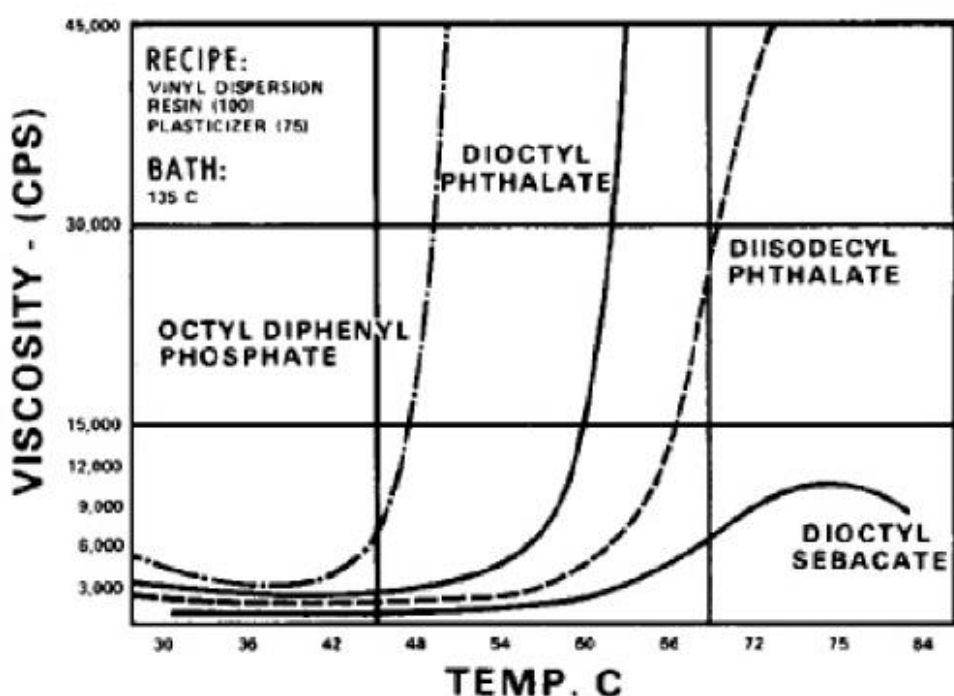


Figure 4 [14] viscosity profiles of plastisols at different temperatures. The dioctyl phthalate profile is of particular interest

However, once the temperature of the plastisol has surpassed 180°C, the gelled PVC begins to melt, decreasing its viscosity to manageable levels. Finally, if the material is once again cooled to below room temperature, it hardens to form an elastic solid with a Shore hardness of approximately 40A.

Knowing these properties, the different 3D printing processes can be evaluated for their suitability.

### 1. Photopolymerisation

Photopolymerisation is an attractive process due to its capability of producing parts with a very high resolution. Indeed, it is possible to cure PVC by applying ultraviolet light. In fact, Eugen Baumann coincidentally discovered PVC due to it polymerising through UV light incidence. However, the effect is not pronounced enough to be viable for a 3D printing application. Furthermore, construction of an SLA printer is comparatively difficult, and the high potential for skin contact with harmful plasticisers is undesirable.

## 2. Binder jet

Unfortunately, binder jet technology is thoroughly unsuitable for this material. As this technology relies on a separate powder and binder, rather than a single material to be cured, P206 cannot be printed using this technology.

## 3. Fused deposition modelling

FDM printers are a reliable option for this material, as they operate by heating a material and depositing it on a platform. As heat is the easiest and most reliable way of causing PVC plastisol to gel, this is deemed to be the most suitable process. Furthermore, the construction of a 3D printer hotend lends itself to conversion from a filament feed to a liquid feed system.

## CNC technology

Computer Numerically Controlled (CNC) machines are similar to regular machine tools, with one major exception. Whereas the normal machine tool would be operated by hand or through a power feed, CNC machines use electronically controlled motors to position the tool/workpiece very accurately. The motors that accomplish this are a special type of electric motor called a stepper motor. Modern 5-axis CNC mills can perform a vast variety of operations at comparatively high feed speeds and with a high degree of accuracy and repeatability. In 3D printing, CNC is used to control the x, y and z axes as well as the extruder motor(s). Fortunately, 3D printers are subjected to very small forces when compared with other machine tools such as lathes or mills.

## Control of motors

Stepper motors are a type of DC motor that responds with a fixed step of rotation for a given electric pulse. This means that by counting the pulses sent to the motor, its angular position can be accurately controlled, up to  $1.8^\circ$ . Finer resolution is possible by using a reducing gear set, at the expense of output speed, or by microstepping the motor. The electronic principle behind driving stepper motors is Pulse width modulation (PWM). This means that a varying voltage (in the shape of a square wave) is sent to the different windings of a stepper motor. The speed and angular displacement of the motor depends on the length of time for which the voltage is on per cycle (Duty cycle, given as a percentage). If visualized on an oscilloscope, this appears as if the peaks of the square waves are widening, hence the term "Pulse Width Modulation". Another electronic system used in the control of Stepper Motors is called an H-Bridge. This is a circuit made up of switches that can change the direction in which the voltage is applied across a motor (this works with DC motors only.). This allows the motor to change direction without rewiring work, manual switching or an expensive gearbox/clutch system. Most 3D printers use stepper motor drivers such as the Pololu A4988 stepper motor driver, or variants thereof.

## Programming

Generally, most CNC machines will be programmed in a language referred to as G-code. This is a form of programming language that can be read by a controller on the machine and be translated into a toolpath for it to follow. G-code for 3D printers is generated by so-called slicer software. This software takes a stereolithography file (.stl file format) and converts it into slices of the desired layer height. The slicer software can also determine such features as fill pattern and wall thickness.

An example of some lines of 3D printer G-code is as follows:

M104 S230  
G28  
G1 X0 Y0 Z5 F8000  
M109 S230

Set hot end temperature to 230°C  
Home all axes (go to maximum endstop position in x, y and z)  
Centre nozzle 5mm above bed  
Wait for hot end to reach 230°C

## Types of FDM printers

### 1. Cartesian

Cartesian 3D printers represent the most commonly used variety of FDM 3D printer. Cartesian 3D printers typically move along three perpendicular axes to achieve movement in three-dimensional space. The advantage of Cartesian printers lies in their mathematical simplicity. In order to go to a predefined point, the Cartesian robot need only translate by a certain distance in X, Y and Z. This, in turn reduces the computational load on the printer's microcontroller.

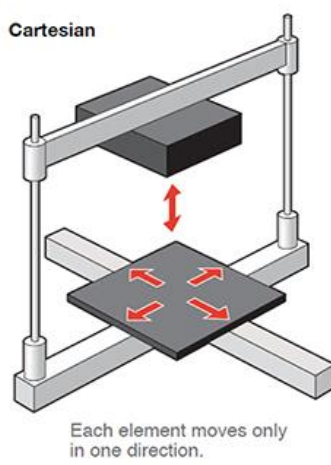


Figure 5 - Cartesian 3D printer

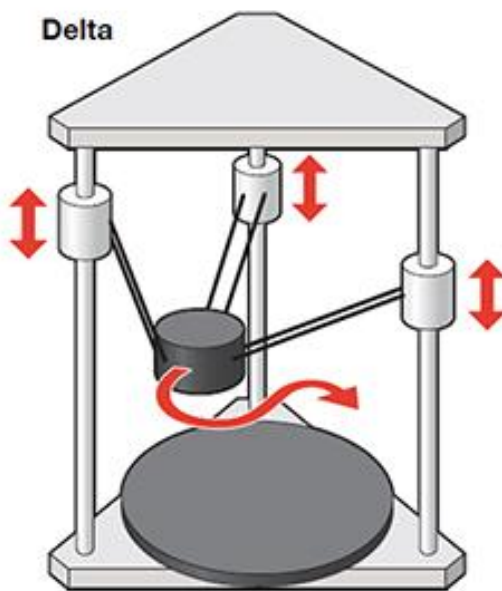


Figure 6 - RepRap Mendelmax 3.0

Additionally, Cartesian printers are easy to source parts for and build with limited resources, making them the primary choice of 3D printer for hobbyists and those looking for a simple to build and easy-to-maintain personal 3D printer. Examples include the RepRap Mendelmax 3.0

### 2. Delta

Delta-type 3D printers have several advantages over classic Cartesian 3D printers. Their design allows the extrusion head to have comparatively little mass, allowing high movement speed and acceleration without causing undue vibrations. Delta-type printers generally feature a circular (as opposed to square) build platform, and also operate in Cartesian coordinate space. They also feature reduced build complexity compared to Cartesian-type printers. However, these advantages come at the cost of greatly increased processor overheads, as the kinematics of the delta printer are considerably more complex than simply translating along the required axes.



Printer head can move in any direction quickly.

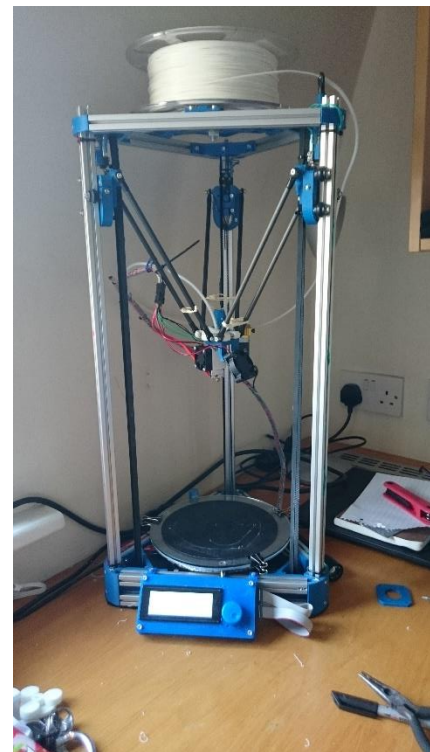


Figure 7 - Delta-type 3D printer

Figure 8 - The RepRap Kossel Mini used for this project

This project was carried out using a RepRap Kossel Mini, the author's personal 3D printer, as a testbed. The Kossel mini has several advantages that facilitate unorthodox modifications. First, a regular Cartesian 3D printer carriage is quite cramped as its extruder motor is placed immediately behind the printer's hot-end. This means that the carriage has a high mass and little room for modification. Conversely, a delta-type 3D printer has a relatively uncluttered end-effector plate at the end of the three linkages (see figure 7). Secondly, as the effector plate "floats" between the linkages, it is easily accessible and is readily modified. As long as the distance between the linkage mounting points remains the same, the effector plate can have effectively any geometry.

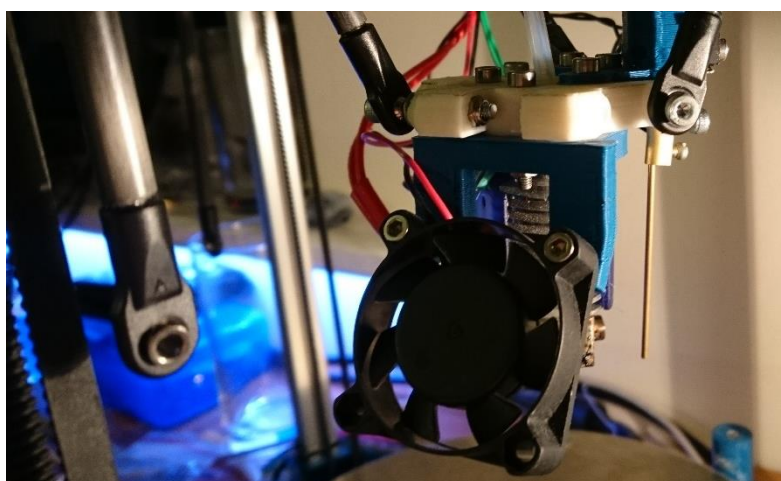


Figure 9 - the conventional hot end in the process of disassembly. Note the disconnected carbon fibre rod on the left.

## Theory of PVC plasticisation

There are three main theories on the mechanism of plasticisation. The first, known as the lubricity theory, characterises the action of a plasticiser as a lubricant between polymer chains which would otherwise have high friction amongst themselves. The theory stipulates that when the polymer is heated to begin the plasticisation, the plasticiser can slip between the polymer chains. Once the polymer has cooled, the plasticiser will facilitate the relative movement of the polymer chains.

Gel theory is a variant of the lubricity theory where the plasticiser dispersed in the PVC matrix simply obscures some of the locations through which the intramolecular forces between polymer chains could act.

As mentioned above, PVC in its near-pure or unplasticised state (uPVC) is rigid at room temperatures, due to the strong attraction between the polymer chains of the material. If the PVC is heated, these chains relax, softening the material and increasing the space between the chains. This space is known as the free volume, and gives rise to the third theory, the “free volume theory”. In free volume theory, the plasticiser spaces the PVC chains apart in much the same way they would at elevated temperatures. In effect, the plasticiser simply lowers the glass transition temperature of the entire material in such a way that the material acts at room temperatures as it would act when heated. <sup>[15]</sup>

There are two main types of plasticisers:

Internal plasticisers actually become a part of the polymer chains themselves and can be defined as a copolymer. Internal plasticisers act by disrupting the orderly nature of the PVC chains, increasing the free volume and thus softening the material and decreasing its glass temperature.

External plasticisers are by far the most common type of plasticiser. Unlike internal plasticisers, which must be added during the polymerisation step of PVC production, external plasticisers can be added to a PVC resin after the fact, thus allowing manufacturers a great deal of freedom when choosing their PVC-P formulation. External plasticisers function by dissolving into the PVC polymer mesh and thereby increasing its free volume. <sup>[16]</sup>

Additionally, plasticisers fall into two further categories – primary and secondary plasticisers. A primary plasticiser is what is imagined as a classical plasticiser. It acts through the mechanisms listed above and is directly responsible for a decrease in hardness and glass transition temperature of the material. In contrast, a secondary plasticiser does not directly act on the polymer but rather on the primary plasticiser in the matrix, binding to it and increasing its effect on  $T_{\text{glass}}$  and material hardness.

## DEHP (Bis(2-Ethylhexyl) Phthalate)

Also known simply as di-ethylhexyl phthalate, DEHP has been the go-to primary plasticiser around the world for the last half-century. It has seen use in PVC products ranging from paints and coatings to toys, buoys and traffic cones as well as in the medical industry, where its good workability and high compatibility with PVC help to make high quality soft PVC. In the EU, DEHP makes up 10% of the total plasticiser market, and 37.1% worldwide. <sup>[17]</sup> DEHP is a low molecular weight orthophthalate with the chemical formula  $C_{24}H_{38}O_4$ , and is classified as reprotoxic (class 1B) under the EU’s REACH (registration, evaluation, authorisation and restriction of Chemicals) regulation. <sup>[18]</sup> As such, DEHP is reaching the end of its life – as it is listed under annex XIV it has a “sunset date” of the 21<sup>st</sup> of February 2015, after which it may only be used for registered purposes. This does not mean that DEHP is going to disappear entirely from medical devices; medical devices regulated by the medical device directive 93/42/EEC are exempt from the REACH program according to article 60(2) of REACH (regulation EC no.

1907/2006). Furthermore, DEHP is also exempt for use in medical packaging by article 17 of regulation 143/2011.

Low-molecular weight phthalates, and DEHP in particular, have been the subject of heavy criticism due to their carcinogenicity and genotoxicity <sup>[19]</sup> and their effect on the sexual development of male rats due to maternal exposure <sup>[20]</sup>. Additionally, a large-scale study conducted in China <sup>[21]</sup> found that heavy phthalate exposure in the environment (as detected by phthalate metabolites in urine) correlates with sperm counts below reference.

### Ethical Issues

The use of plasticisers is effectively unavoidable if PVC is to continue being used as a material in any application other than for construction. PVC is also a superior material to its precursors latex and natural rubber, with between 8 and 12% of all healthcare workers and between 1% and 6% of the general population showing allergic symptoms to latex. This situation keeps PVC in such broad use despite the toxicity of some plasticisers. Fortunately, since the discovery of the harmfulness of Phthalates in the 1980s, a large variety of alternatives have been developed which promise equal performance to DEHP without the ill effects. TOTM (Trioctyl Trimellitate) and DINCH (1,2-cyclohexane dicarboxylic acid diisononyl ester) are increasingly replacing DEHP to the point where it is soon to be extinct for most applications; in particular, the medical device industry intends to move away from all phthalates in order to avoid the negative publicity associated with them, despite the fact that in the EU they are not obliged to suspend the use of DEHP, a trend that can be seen by the use of DEHP in the EU compared to worldwide, making up just 10% of Europe's plasticiser market in comparison to 37% of the global market.

Unfortunately, there is also controversy surrounding the alternative plasticisers. Although there has been a heavy push to reduce the use of phthalates, the alternatives touted for medical devices, such as TOTM, have comparatively little data on their actual toxicity. While the existing data seems to suggest the safety of the material in terms of its lack of reprotoxicity <sup>[22]</sup>, other forms of toxicity such as carcinogenicity and genotoxicity have not been sufficiently evaluated to eliminate all risk. Furthermore, while Eckert et al found that TOTM does not migrate into blood as heavily as DEHP, other plasticisers show significantly higher rates of migration.

A study conducted in Spain in 2007<sup>[23]</sup> used FTIR spectroscopy to compare the migration profiles of Citrates, Adipates and Phthalates. Their results showed that Phthalates have the slowest rate of migration of the three, followed by citrates. Adipates in comparison leached from the PVC material most quickly.

While it should be noted that these plasticisers are less toxic, their increased rate of migration may still prove to be a problem if the material accumulates in a person over time.

# Project Management

## First Semester

Fortunately, as this project was self-conceived, I was able to begin working immediately after returning from work placement over the summer of 2015. The winter semester began by planning out the initial stages of the project, consisting of the following approximate schedule:

1. Literature review	August-September
2. Design of Experiments	October
3. Testing	Late October
4. Systematic Design	November / December
5. Semester 1 Report	December

In order to remain on track for the duration of the semester, this data was entered into ProjectLibre to create a Gantt chart running the duration of the semester, starting on the 7<sup>th</sup> of September 2015.

		Name	Duration	Start	Finish
1		Literature Review	20 days	07/09/15 08:00	02/10/15 17:00
2		Analysis and comparison of 3D printing process	20 days	07/09/15 08:00	02/10/15 17:00
3		Design of Experiments	7 days	05/10/15 08:00	13/10/15 17:00
4		Building of Test rig	7 days	14/10/15 08:00	22/10/15 17:00
5		Performance of testing	7 days	23/10/15 08:00	02/11/15 17:00
6		Systematic Design	14 days	03/11/15 08:00	20/11/15 17:00
7		Further Research	14 days	23/11/15 08:00	10/12/15 17:00
8		Semester 1 report	7 days	11/12/15 08:00	21/12/15 17:00

Figure 10 - Semester 1 Project Schedule

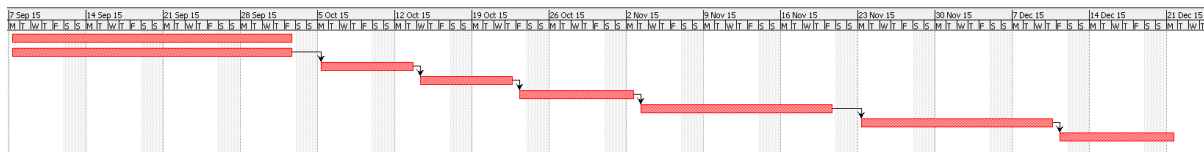


Figure 11 - Semester 1 Gantt Chart

During Semester 1, it became clear that other obligations as well as the required study were beginning to encroach on the project's timeframes. In fact, as time progressed, the project slipped about a month behind time. The semester progressed as follows:

1. Literature review	August-September
2. Design of Experiments	October
3. Testing	Late October
4. Systematic Design	Early December
5. Semester 1 Report	Early January

Fortunately, enough slip time was included in the initial plan to make up for these losses – furthermore, an extension was granted to the class in order to free up time for exam study.

## Second Semester

The time plan for first semester built on a combination of the plan for first semester and the deferred hand-up date on the 5<sup>th</sup> of January, factoring in 5 days of free time.

		Name	Duration	Start	Finish	Predecessors
1		Literature Review	20 days	07/09/15 08:00	02/10/15 17:00	
2		Analysis and comparison of 3D printing processes	20 days	07/09/15 08:00	02/10/15 17:00	
3		Design of Experiment	7 days	05/10/15 08:00	13/10/15 17:00	2
4		Construction of test rig	7 days	14/10/15 08:00	22/10/15 17:00	3
5		Testing	7 days	23/10/15 08:00	02/11/15 17:00	4
6		Systematic Design	14 days	03/11/15 08:00	20/11/15 17:00	5
7		Further Research	14 days	23/11/15 08:00	10/12/15 17:00	6
8		Semester 1 report	7 days	11/12/15 08:00	21/12/15 17:00	7
9		prototyping of feed system	14 days	10/01/16 08:00	28/01/16 17:00	8
10		assembly and testing of feed system	7 days	29/01/16 08:00	08/02/16 17:00	9
11		calibration of feed system	7 days	09/02/16 08:00	17/02/16 17:00	10
12		integration of feed system into 3D printer	7 days	18/02/16 08:00	26/02/16 17:00	11
13		3D printer firmware and electronic modification	14 days	29/02/16 08:00	17/03/16 17:00	12
14		comparison of 3D printed and conventional material	14 days	18/03/16 08:00	06/04/16 17:00	13
15		analysis of data and recap of project	7 days	07/04/16 08:00	15/04/16 17:00	14
16		Further Research	7 days	18/04/16 08:00	26/04/16 17:00	15
17		creation of final report	7 days	27/04/16 08:00	05/05/16 17:00	16

Figure 12 - time plan for first and second semester

(Note that the Gantt chart is not included here, as work was purely linear and dependent on the preceding work to be completed.)

Second semester began on schedule, about a week after the first semester report was turned in. Work began with the prototyping of the feed system pump. Unfortunately, some issues were encountered with motor torque, forcing a redesign of the feed pump. The necessary adjustments were made to the system and work progressed. It was then found during the calibration stage that the feed pump (an entirely 3D printed mechanism) suffered from excessive backlash. An alternative pump was purchased from a Dutch supplier and this pump was calibrated. Following these two setbacks, the project was able to win back a little time, with the project considered complete on the 10<sup>th</sup> of May 2016, 5 days after the scheduled completion date.

As the timetable in second semester is structured differently to that of first semester, lecture and additional study time were not as severe a problem as in first semester, and no deadline extensions were necessary.

## Initial Testing

Purpose of testing:

To investigate the behaviour of the PVC when extruded through a conventional 3D printing extruder, as well as to gain an insight into the pressures and temperatures required to process the material in this manner.

Apparatus:

Experimental Setup

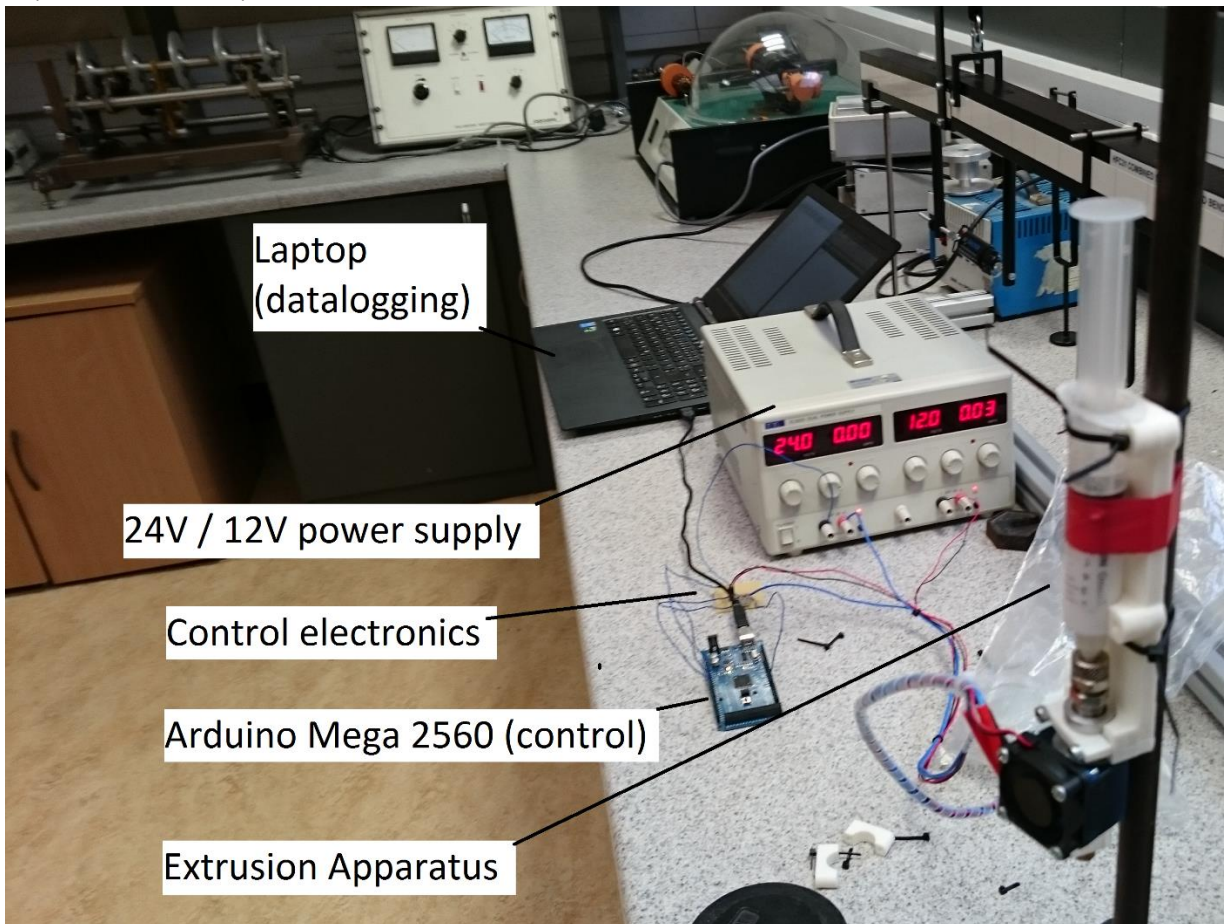


Figure 13 - Bench Testing

The photograph above shows the experiment between test runs. In the foreground the extruder can be seen filled with PVC and mounted to a stand, ready for weights to be applied on the syringe plunger, as well as the power supply and control circuitry. Note the Current reading on the 24V supply: 0 Amps are being supplied, meaning the Arduino has not yet switched on the heating element. The 12V supply is providing power for the cooling fan, which is run continuously.

## Extruder

The extruder used for this experiment consisted of a syringe attached to a modified e3d v6 Extruder, with a 0.4mm nozzle, as pictured below:

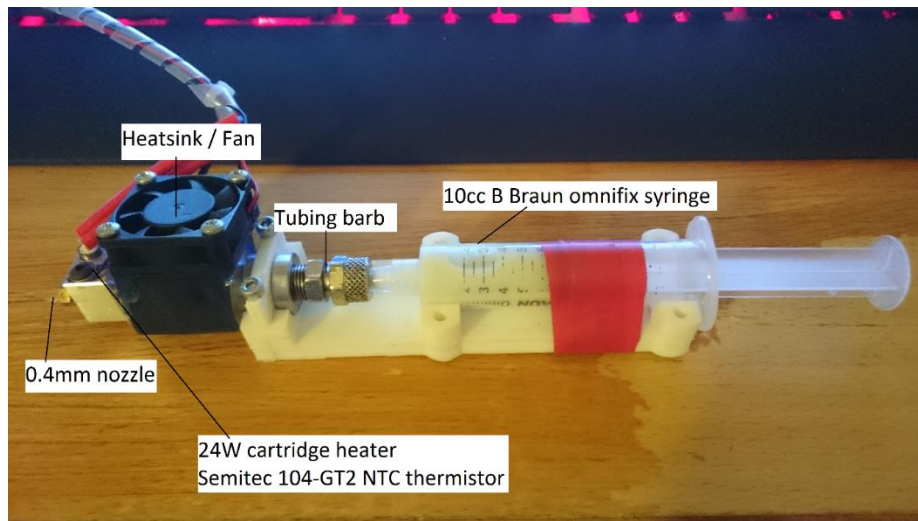


Figure 14 - Extruder test rig

The entire apparatus is mounted on a 3D-printed bracket. The syringe, containing the PVC plastisol, was connected to the hotend via a hose barb and a short length of 6mm silicone tubing. A bracket was 3D printed in ABS to hold all parts in alignment. During the experiment, weights are applied to the plunger until cured ABS begins to be extruded from the nozzle. The required pressure can then be calculated by knowing the internal diameter of the syringe and the force applied to it.

The inner diameter of the syringe was measured as 15.75mm.

The e3d v6 hotend (pictured below) was chosen for this experiment because of its robust aluminium design and open-source community support, meaning that all required documentation is easily available. Furthermore, the aluminium body meant that it was quite easy to simply bore out and thread the extrusion channel to attach a hose fitting. Beginning with a commonly-used platform like the e3d series of hotends also allows a reduced design complexity when integrating the nozzle into an existing 3D printer.

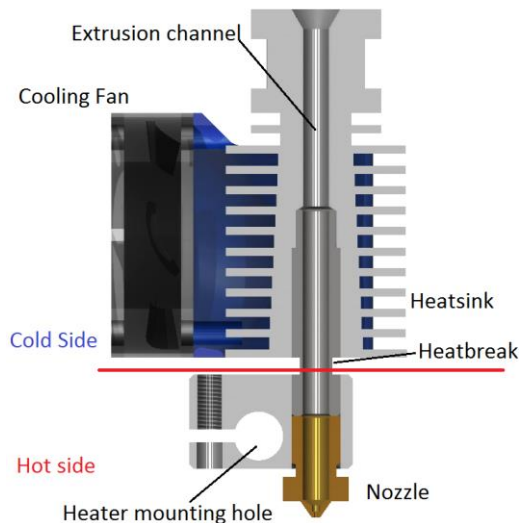


Figure 15 - e3d v6 hotend

## Temperature Control

In order to maintain the hotend at the desired temperature, a PID controller was implemented on an Arduino Mega 2560, using the following code:

```
#include <PID_v1.h>                                //PID library
#include <math.h>                                    //Math library

double Setpoint, Input, Output;                      //declare variables used in the code

double Thermistor(int RawADC){                     //declare the function that reads the
    double temp;                                     //temperature from the thermistor
    temp= log(9600.0*((1024.0/RawADC-1)));          //using the Steinhart-Hart equation
    temp=1/(0.0008104849864+(0.0002115244184+(0.00000007098035250*temp*temp)*
    *temp));                                         //using the Steinhart-hart coefficients
    temp=temp-273.15; //convert absolute temperature into degrees celsius
    return temp;
}

//create a PID controller, defining input, output, setpoint, Kp, Ki and Kd,
set to direct mode
PID tempPID(&Input, &Output, &Setpoint, 21.28, 2.37, 47.76, DIRECT);

void setup() {
Serial.begin(9600);                                //begin Serial communication
tempPID.SetMode(AUTOMATIC); //set PID to run automatically
Setpoint=0;                                         //initialise setpoint to 0 (off)
}

void loop() {
    Input = Thermistor(analogRead(A0)); //PID input is the current temperature

    tempPID.Compute();                            //calculate the PID's output
    analogWrite(3, Output);                      //write the output as PWM to one of
the digital pins

    Serial.print(Setpoint);                      //serial outputs for datalogging
    Serial.print(",");
    Serial.print(Input);
    Serial.print(",");
    Serial.println(Output);
    if(Serial.available() !=0){                  //if there is a non-zero integer in the
incoming stream
        Setpoint=Serial.parseInt();             //set the setpoint to the integer
    }
    delay(250);                                //repeat 4 times per second
}
```

The Steinhart-Hart equation referenced in the code comments is the following equation:

$$\frac{1}{T} = A + B * \ln(R) + C [\ln(R)]^3$$

The equation models the behaviour of NTC (negative temperature coefficient) thermistors. The variables represent the following:

- T is the absolute temperature in Kelvin
- R is the resistance of the thermistor in Ohms
- A, B and C are coefficients individual to the resistor used. These can be acquired from the Thermistor's documentation.

In this case, A, B and C were found by examining the manufacturer datasheet for the Semitec 104-GT2 thermistor found at <http://www.atcsemitec.co.uk/gt-2-glass-thermistors.html>. Considering the intended temperature range of the extruder would be between room temperature and approximately 250°C, the following resistance values were used:

T<sub>1</sub>      0°C      353.7kΩ

T<sub>2</sub>      100°C    5.556kΩ

T<sub>3</sub>      250°C    0.1740kΩ

Plugging these into the matrix calculation for A, B and C:

$$\begin{matrix} & & & & 1 \\ 1 & \ln(353700) & (\ln(353700))^3 & A & \frac{0 + 273.15}{1} \\ 1 & \ln(5556) & (\ln(5556))^3 & * B & \frac{100 + 273.15}{1} \\ 1 & \ln(174) & (\ln(174))^3 & C & \frac{250 + 273.15}{1} \end{matrix}$$

Solving the above yields the following values:

$$\begin{aligned} A &= 0.8104849864 * 10^{-3} \\ B &= 2.115244184 * 10^{-4} \\ C &= 0.7098035250 * 10^{-7} \end{aligned}$$

For example, a resistance of 439Ω will correspond to a temperature of:

$$\begin{aligned} \frac{1}{T} &= (0.8104849864 * 10^{-3}) + (2.115244184 * 10^{-4})(\ln(439)) \\ &\quad + (0.7098035250 * 10^{-7})(\ln(439))^3 \end{aligned}$$

$$T = 473.1502^\circ K$$

$$T = 200.0002^\circ C$$

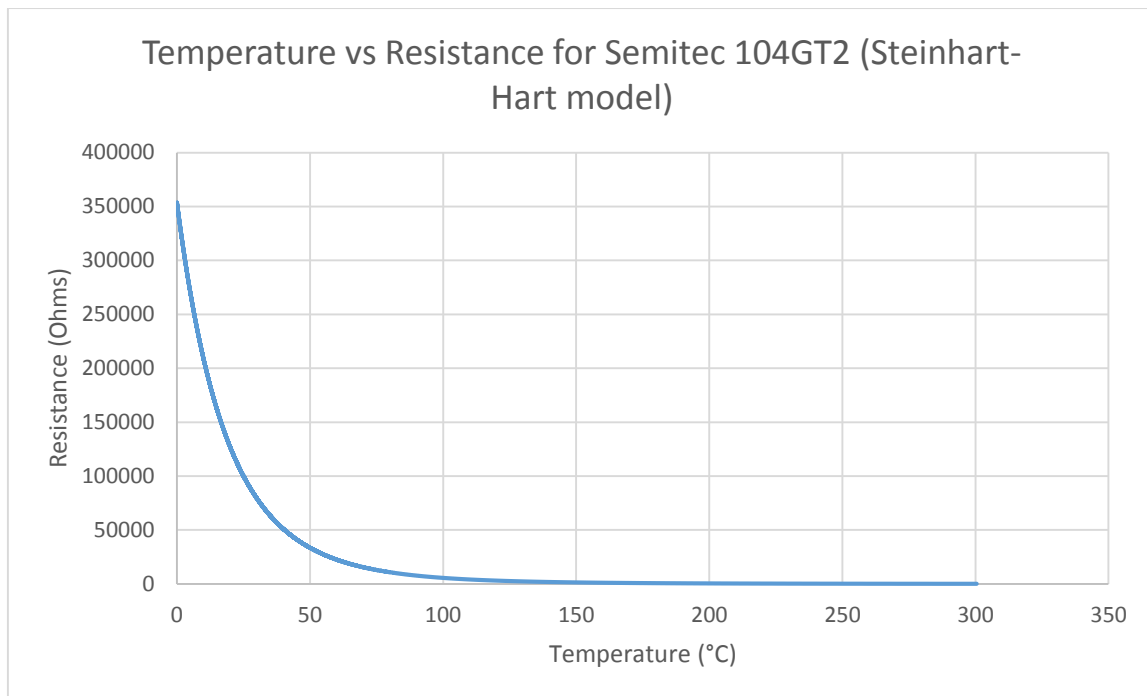
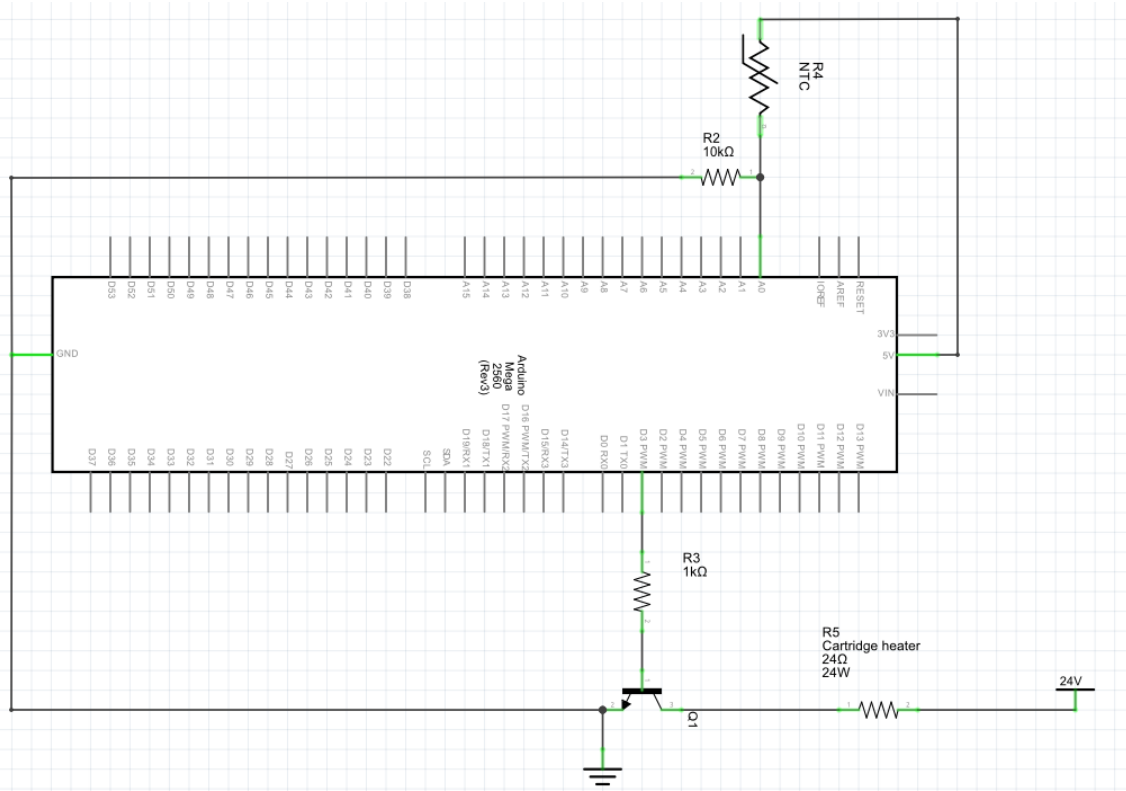


Figure 16 - Steinhart-Hart model of Semitec 104GT2 thermistor

## Circuitry

The extruder was powered using a 24V power supply unit borrowed from the electronic engineering department. In order to measure the temperature of the extruder as well as regulate its power output, the following circuit was designed:



*Figure 17 - schematic of temperature control circuit*

In effect, there are two separate circuits in this schematic. The first is a voltage divider where R2 is a 10kΩ resistor and R4 is the NTC thermistor, allowing changes in the thermistor's resistance to be measured as voltage changes by the Arduino. However, when measured with an Extech EX330 multimeter, the resistor was found to be closer to 9600Ω. In order to prevent errors due to this discrepancy, the 9600Ω resistance was used in the voltage divider calculation.

In order to calculate the output of the voltage divider, the following formula is used:

$$V_o = V_i \frac{R_2}{R_{Thermistor} + R_2}$$

$$V_o = \frac{5 * 9600}{R_{Thermistor} + 9600}$$

So, if the Arduino reads 2.5 V as the output of the voltage divider, then

$$\begin{aligned} 2.5 &= \frac{48000}{R_{Thermistor} + 9600} \\ 2.5R_{Thermistor} + 24000 &= 48000 \\ R_{Thermistor} &= 9600\Omega \end{aligned}$$

Which, according to the Steinhart-Hart model of the 104GT2 corresponds to a temperature of 83.38°C.

The second circuit consists of a TIP 121 Darlington-type NPN power transistor. These transistors are capable of regulating up to 80V at 5A, and allow the Arduino to rapidly switch the heater on and off using a PWM signal, thus allowing it to regulate the heater's power output in response to the changing output of the PID controller.

The circuit was then assembled on a piece of prototyping board and soldered in as pictured below:

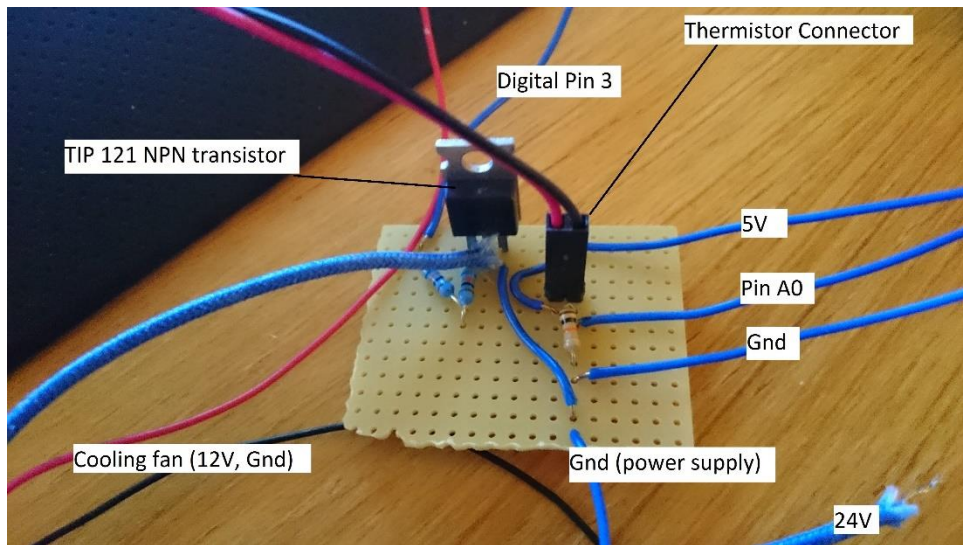


Figure 18 - circuit on prototyping board

## Procedure

Before beginning the testing, the force of friction of the syringe had to be determined. In order to do this, the syringe was filled with air and the connector to the extruder was disconnected. Weights were added on the syringe plunger in 2N increments until the plunger began to move, at which point, the total force acting on the plunger was recorded. This was repeated a total of 3 times, and the average force of resistance was calculated. The results were tabulated as below:

Syringe resistance			
Attempt 1 (N)	Attempt 2 (N)	Attempt 3 (N)	Mean (N)

PVC P206 begins to gel rapidly at 180°C and above. It also begins to degrade and discolour very rapidly above 210°C. Therefore, it was decided to examine the following temperatures:

Temp (°C)	Attempt 1 (N)	Attempt 2 (N)	Attempt 3 (N)	Mean (N)	Mean Pressure (Pa)	Mean Pressure (Bar)
210						
200						
190						
180						

The extruder was connected to the power supply and the control circuitry. After establishing contact to the Arduino via serial connection and beginning to log the data to the attached PC, the temperature of the extruder was set to the level desired for the test run. The air was manually purged from the extrusion channel by pressing down the plunger by hand until PVC began to be extruded from the nozzle, at which point no more force was exerted on the plunger by hand. Once the flow of extruded PVC stopped, weights were added on top of the plunger in 2N increments until a steady stream of PVC could be observed being extruded from the nozzle of the extruder. At that point, the total force on the plunger was recorded.

After three attempts for each temperature setting, the mean was calculated. The mean pressures in Pa and in Bar were subsequently calculated.

Example calculation

Syringe diameter=15.75mm

$$\text{Syringe cross-sectional area } (A = \frac{\pi d^2}{4}) = 0.000194828 \text{ m}^2$$

$$\text{Pressure} = \frac{\text{Force}}{\text{Area}}$$

If F=3.33N and A=19.4828\*10-4 m2

$$P = \frac{3.33}{0.000194828} = 17109.12 \text{ Pa} = 1.71 \text{ Bar}$$

## Results

Syringe resistance			
Attempt 1 (N)	Attempt 2 (N)	Attempt 3 (N)	Mean (N)
18	20	18	18.67

Raw Data				
Temp (°C)	Attempt 1 (N)	Attempt 2 (N)	Attempt 3 (N)	Mean (N)
210	20	24	22	22.00
200	24	26	30	26.67
190	30	32	34	32.00
180	40	38	42	40.00

Readings corrected for friction						
Temp (°C)	Attempt 1 (N)	Attempt 2 (N)	Attempt 3 (N)	Mean (N)	Mean Pressure (Pa)	Mean Pressure (Bar)
210	1.33	5.33	3.33	3.33	17109.12	<b>1.71</b>
200	5.33	7.33	11.33	8.00	41061.90	<b>4.11</b>
190	11.33	13.33	15.33	13.33	68436.49	<b>6.84</b>
180	21.33	19.33	23.33	21.33	109498.39	<b>10.95</b>

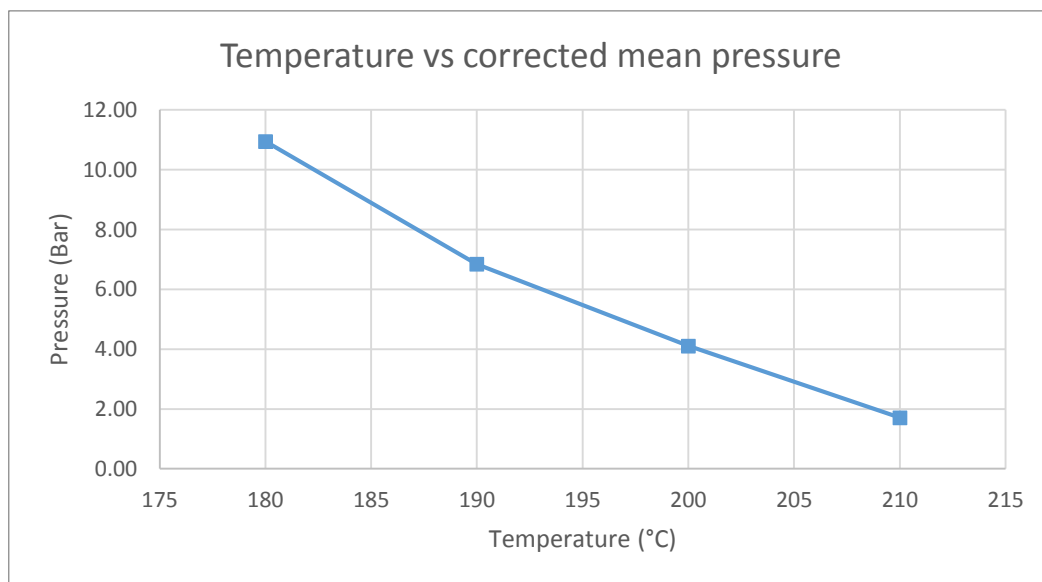


Figure 19 - Graph of Temperature vs corrected mean pressure

## Temperature datalogs

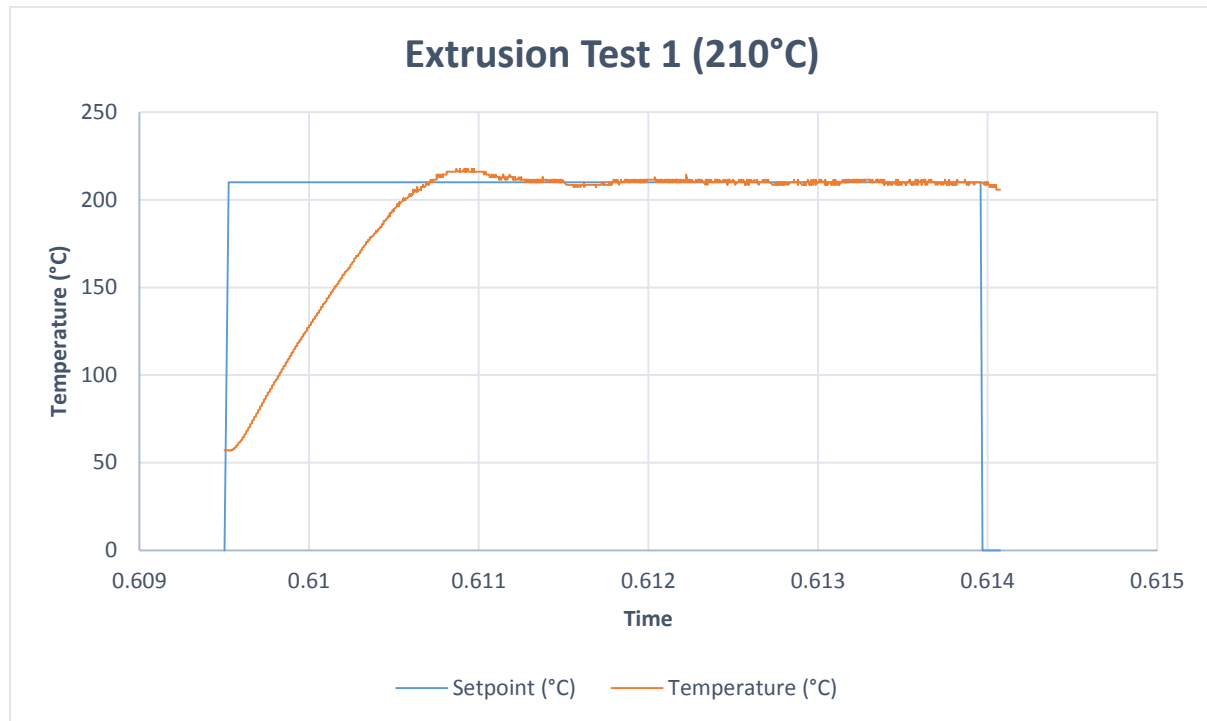


Figure 20 - temperature profile, climbing to 210°C

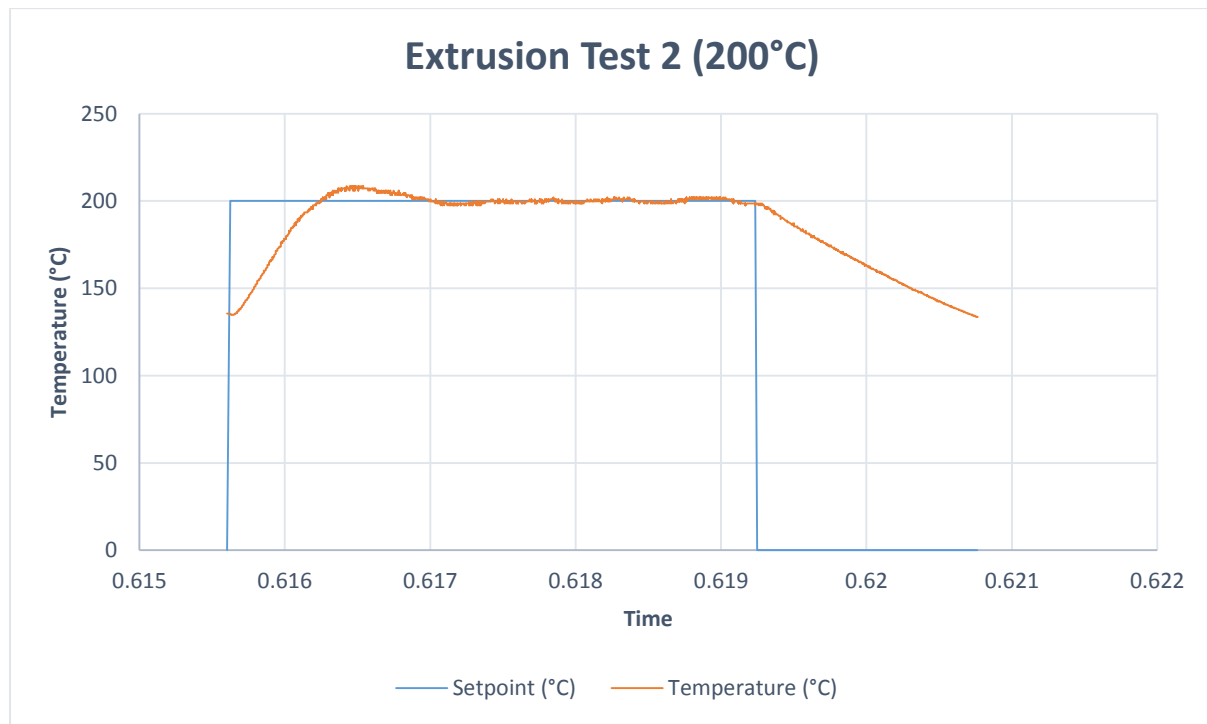


Figure 21 - temperature profile, climbing to 200°C

## Discussion

The data acquired shows that the ideal temperature for the extrusion of the PVC is between 200°C and 210°C, as at these temperatures the PVC overcomes its most viscous phase very quickly and transfers from the viscous gelation phase to the less viscous molten thermoplastic phase. It should be noted however that if the PVC is left for too long at these temperatures, the PVC starts to break down and undergoes degradation by dehydrochlorination, causing the otherwise clear PVC to become yellowed. This implies that feed rates will need to be relatively high in order for the printer to be able to print without “burning” the material being printed.

Furthermore, it should be noted that the syringe used for this experiment had already aged somewhat, and lost its preapplied siliconisation. This meant that the syringe was far stiffer to operate than normal, leading to the relatively high resistance of the empty syringe. While the results were corrected for syringe friction, this factor may have influenced the results by simulating higher extrusion pressure than what is necessary in reality.

In hindsight, this experiment should have been carried out by having a tensile tester compress the plunger both to determine the resistance of the syringe as well as the force required to extrude the material during the test runs. The testing may be carried out in the next semester using this approach.

As it stands, however, the acquired data is deemed sufficient to provide a ballpark estimate of the pressure requirements a prospective extrusion system will have to provide.

## Systematic Design

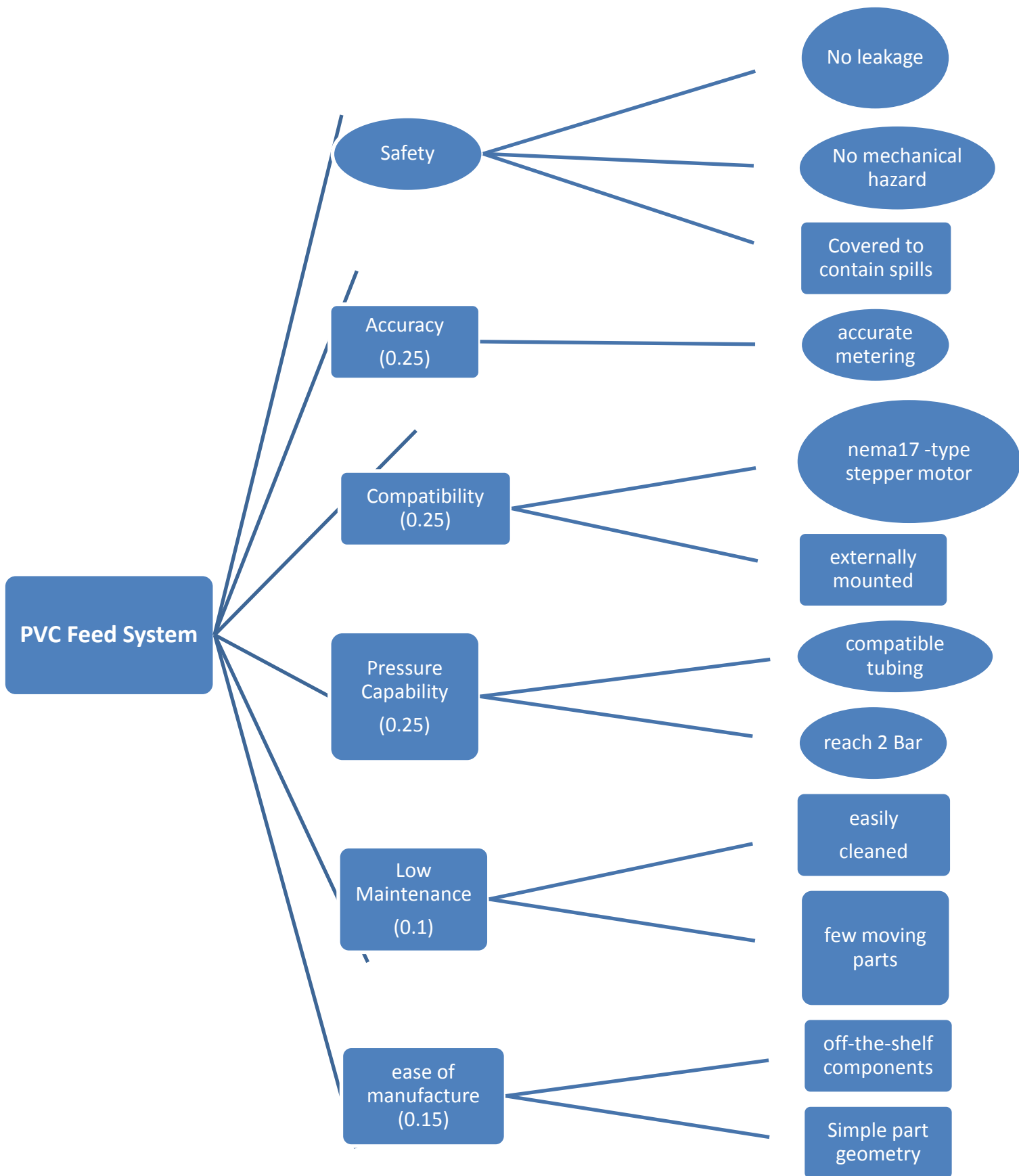
While the extruder used in the experiment described in this report can be used for the final execution of the 3D printer, a feed system must be designed to provide a constant, pressurised flow of liquid PVC plastisol. This feed system will have to be capable of accurately metering the flow of material to the extruder nozzle, as well as being compatible with the printer's control electronics.

### List of primary objectives

The first step in systematic design is to establish the primary objectives that the system needs to fulfil, and to compare these objectives using a pairwise comparison chart to establish their importance in relation to each other. The chart assigns weights to the individual objectives, allowing a metric to be created in order to compare potential designs.

1. Accuracy and precision of metering
2. Compatibility with control electronics
3. Capable of attaining the required extrusion pressures at 210°C
4. Low-maintenance
5. Ease of manufacture

	Accuracy	Compatibility	Pressure Capability	Low maintenance	Ease of manufacture	Total
Accuracy	x	0.5	0.5	1	1	3
Compatibility	0.5	x	0.5	1	1	3
Pressure Capability	0.5	0.5	x	1	1	3
Low maintenance	0	0	0	x	1	1
Ease of manufacture	0	0.5	0	1	x	1.5



The objectives and constraints tree allows the establishment of secondary objectives and requirements. In order to easily distinguish constraints from objectives, constraints are located in the oval shapes, while objectives are inside rectangles. Constraints differ from objectives in that they must be met for the design to be viable.

### Possible solutions

The design problem stated above has only a select few solutions, all of which amount to some variation of positive displacement pump. It was therefore decided to compare a set of five possible designs on their merits using the metrics arrived at in the pairwise comparison chart.

The five chosen pumps were:

1. Syringe driver:



Figure 22 - Syringe driver

2. Peristaltic pump:



Figure 23 - peristaltic pump

3. Progressive cavity pump



Figure 24 - progressive cavity pump

4. Gear pump

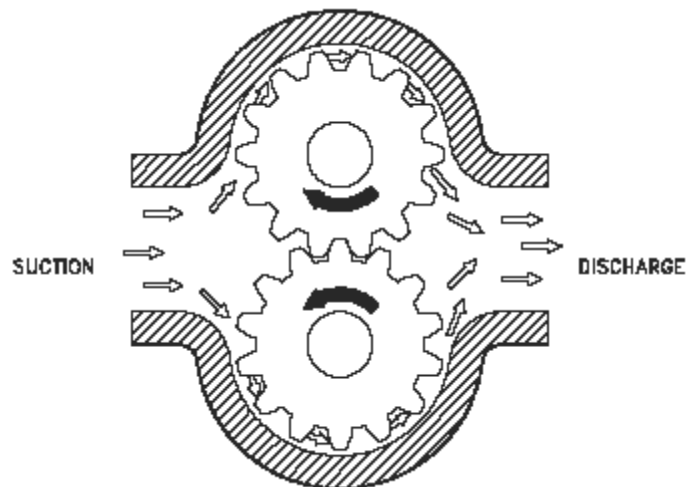


Figure 25 - gear pump

5. Lobe pump

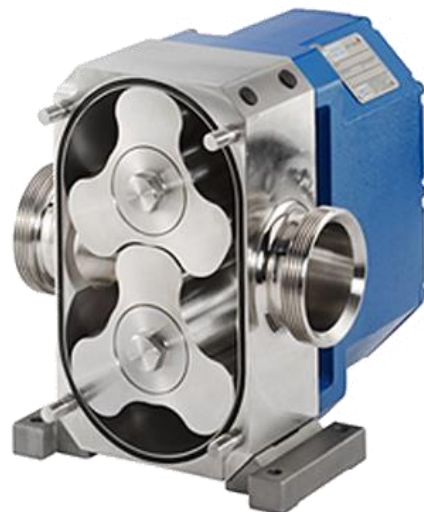


Figure 26 - lobe pump

## Metrics

Metric rating tables are a balanced and unbiased way to compare designs in order to pick the most suitable design. The primary objectives arrived at earlier in the design process are assigned a range of values between 0 and 100. Each design is rated by the degree to which it satisfies the primary objective. These ratings are then weighted by the totals from the pairwise comparison chart.

### Metrics tables

#### 1. Safety

Rating	Description
100	Very Safe
70	Safe
30	Unsafe
0	Dangerous

#### 2. Accuracy and precision of metering

Rating	Description
100	Very accurate
70	Accurate
30	Moderately accurate
0	Inaccurate

#### 3. Compatibility with control electronics

Rating	Description
100	Compatible
70	Compatible with some modification
30	Compatible with major modification
0	Incompatible

#### 4. Capable of attaining the required extrusion pressures at 210°C

Rating	Description
100	Meets required pressures
0	Cannot reach pressures

#### 5. Low-maintenance

Rating	Description
100	Maintenance-free
70	Low maintenance
30	Needs regular maintenance
0	High maintenance

## 6. Ease of manufacture

Rating	Description
100	Very easily manufactured
70	Easily manufactured
30	Manufacturable
0	Unfeasibly difficult

Design choice

Design	Safety	Accuracy	Compatibility	Pressure	Low-maintenance	Ease of manufacture	Total	Weighted total
Syringe driver	70	30	100	100	30	100	430	1080
<b>Peristaltic pump</b>	<b>100</b>	<b>70</b>	<b>100</b>	<b>100</b>	<b>30</b>	<b>100</b>	<b>500</b>	<b>1290</b>
Progressive cavity pump	100	100	30	100	70	0	400	1060
Gear pump	100	100	30	100	70	30	430	1105
Lobe pump	100	100	30	100	70	30	430	1105

As can be seen from the table above, the peristaltic pump is the only truly feasible option, with an unweighted score of 500 and a weighted score of 1290.

The peristaltic pump is ideal for a number of reasons:

- It is very easy to manufacture with off-the-shelf components
- It features few moving parts
- It provides a safe separation between the user and the PVC plastisol, as the plastisol never leaves its tubing
- It can easily reach the pressures required to extrude the PVC.
- It can be designed to be powered by a NEMA 17-type stepper motor with no modification

## Peristaltic Pump Design

### Calculations

To achieve a printing speed of 100mm/s (0.1 m/s) with a 0.4mm nozzle:

Cross-sectional area of the nozzle:

$$A = \frac{\pi d^2}{4} = \frac{\pi (0.4 * 10^{-3})^2}{4} = 1.2566 * 10^{-7} m^2$$

With a flow velocity of 0.1 m/s, this corresponds to a volumetric flow rate of:

$$Q = Av = 1.2566 * 10^{-7} (0.1) = 1.2566 * 10^{-8} m^3/s$$

$$1.2566 * 10^{-8} * 1 * 10^6 = 0.0126 * 60 = 0.7539 ml/min$$

For a peristaltic pump:

$$Q \text{ in } \frac{ml}{minute} = \text{volume of occluded tubing} * \text{number of rollers} * \text{pump rpm}$$

The tubing has an ID of 3.5 mm, and is occluded along an arc of 271° with a radius of 32.5mm

Arc length

$$L = \frac{n}{360} * 2\pi r$$

$$L = \frac{270}{360} * 2 * \pi * 32.5 * 10^{-3} = 0.153m$$

Volume of the tubing

$$V = \frac{\pi d^2}{4} L = \frac{\pi * (3.5 * 10^{-3})^2}{4} * 0.153 = 1.4720 * 10^{-6} m^3 = 1.472 ml$$

Therefore, the pump must rotate at:

$$RPM = \frac{Q}{V * \text{no of rollers}} = \frac{0.7539}{1.472 * 3} = 0.171 RPM$$

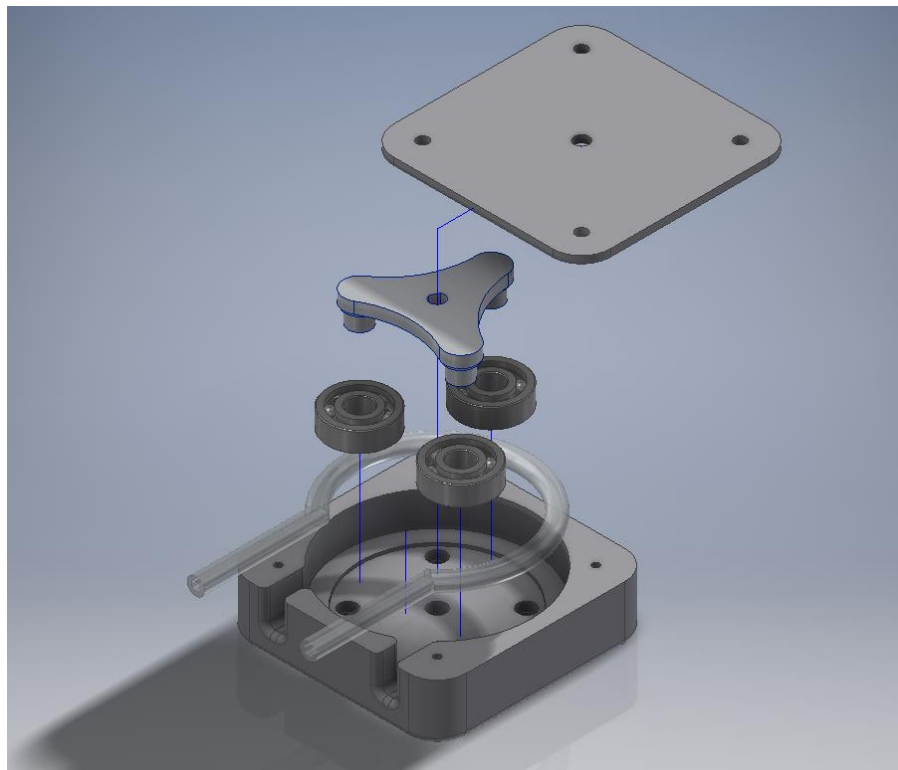


Figure 27 - first iteration of peristaltic pump

The final design consists of a 3-roller peristaltic pump driven by a NEMA 17 stepper motor. The pump uses very common SKF 608zz bearings as rollers to compress the tubing.



Figure 28 - 3D printed prototype, assembled with tubing and NEMA 17 stepper motor

## Testing of initial design

In order to test the initial design, the stepper motor was connected to a Pololu A4988 stepper motor driver mounted on the 3D printer's main board. The motor was then sent 5000 steps. The A4988 was set to 1/16<sup>th</sup> microstepping mode by connecting 5V jumpers to the MS1, MS2 and MS3 pins, pictured below.

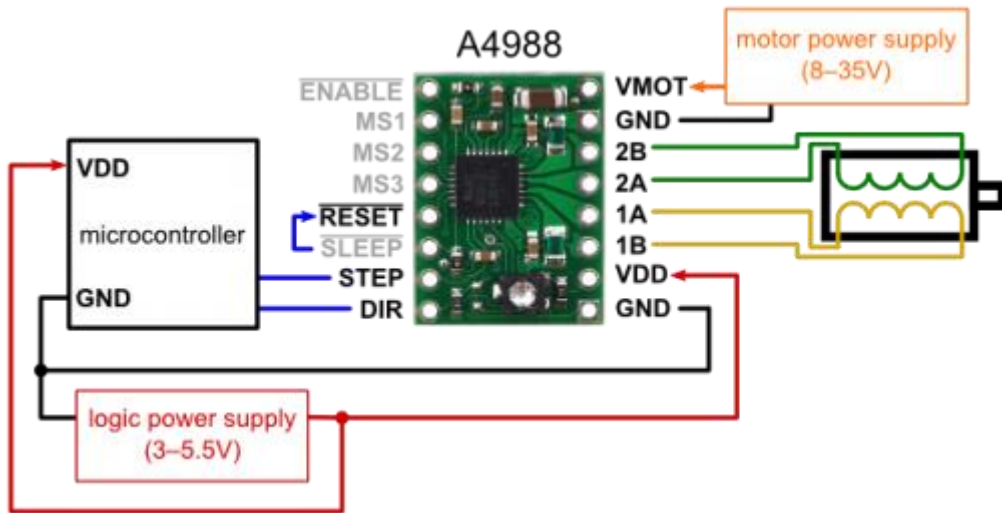


Figure 29 - A4988 stepper motor driver connection diagram

Microstepping mode allows the motor to perform at a much greater step resolution. The NEMA 17 stepper motors used for the RepRap Kossel Mini Delta printer have a base resolution of 1.8° per step, or 200 steps per revolution. In 1/16<sup>th</sup> microstepping mode, the motor can achieve 3200 steps per revolution (200\*16), or 0.1125° per step.

While this technique increases the printer's resolution, it also decreases the torque the motor can provide.

Initial testing showed that the peristaltic pump required far more torque to rotate than the stepper motor could provide even in direct step mode. As a result, the peristaltic pump had to be redesigned.

## Peristaltic pump redesign

There were a number of possibilities to increase the stepper motor's applied torque.

Firstly, a larger NEMA 17 stepper motor could be used. NEMA 17 motors are specified only by the diameter of their mounting flange on the shaft side; their length is not standardised, and as a result it is possible to purchase "triple stack" stepper motors. These motors require a much higher current per to operate (around 2A), but provide considerably more torque (65Ncm, compared to 47Ncm for a regular NEMA 17). This increased current draw means that for such a large motor to be used, the A4988 stepper motor driver must be replaced with a high-current driver, such as the DRV8825.

Secondly, the pump could be redesigned to feature a reduction gearbox to increase the torque output of the motor. Since speed is not an issue (calculated as 0.17 RPM on page 34), this was a viable option.

It was decided to employ both approaches; a larger stepper motor was used, and a reduction gearbox was designed to drive the peristaltic pump.

## Gearbox design

One of the main design criteria of the peristaltic pump during the systematic design phase was ease of manufacture. In keeping with this criterion, it was decided that the peristaltic pump was to be 3D printed. As it is difficult to print and align shafts made of ABS or PLA due to the limitations of the 3D printing process, A planetary (epicyclic) gearbox was chosen for the purpose of this design.

Epicyclic gearing consists of one or more planet gears meshing with both a sun and an annular gear, as shown in fig. 30:

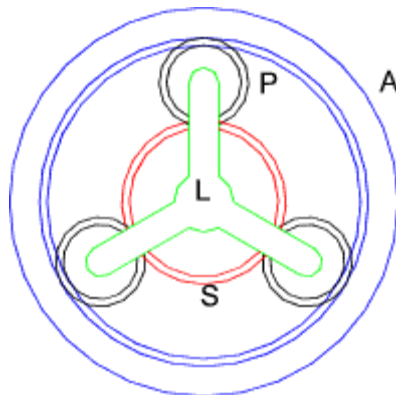


Figure 30 - epicyclic gearing

In order to achieve a space-efficient layout, it was decided to use the sun gear as the input gear, and the planet carrier (labelled L in fig. 30) as the output, with the rollers of the peristaltic pump mounted to the exterior of the carrier. The annular gear would be part of the casing. Additionally, a reduction of 5:1 was decided.

For a planetary gearset in “planetary arrangement”, i.e. power transmission from sun to planet carrier, with a fixed annulus:<sup>[24]</sup>

$$\frac{R_s}{R_L} = 1 + \frac{N_A}{N_s}$$

Where  $R_s$  is the number of revolutions of the sun gear,  $R_L$  is the number of revolutions of the planet carrier,  $N_A$  is the number of teeth in the annulus and  $N_s$  is the number of teeth on the sun gear.

Assuming a 12-tooth sun gear, and a 5:1 reduction

$$\frac{5}{1} = 1 + \frac{N_A}{12}$$

$$N_A = 48 \text{ teeth}$$

In order for the sun, annulus and planet to mesh properly, the following rule must be observed:

$$N_p = \frac{N_A - N_s}{2}$$

In this case,

$$N_p = \frac{48 - 12}{2} = 18 \text{ teeth}$$

Finally, in order for the planet gears to all mesh correctly, the sum of the teeth in the sun and annulus must be evenly divisible by the number of planets. In this case,

$$48 + 12 = 60$$

Leaving the option to use 1, 2, 3, 4 or even 5 gears. However, the design becomes very simple when three gears, spaced  $120^\circ$  apart are used. Employing three gears (as opposed to two) ensures that the mechanism is self-centering due to the constraints of four circles in tangential contact with an annulus.

The following design was arrived at:

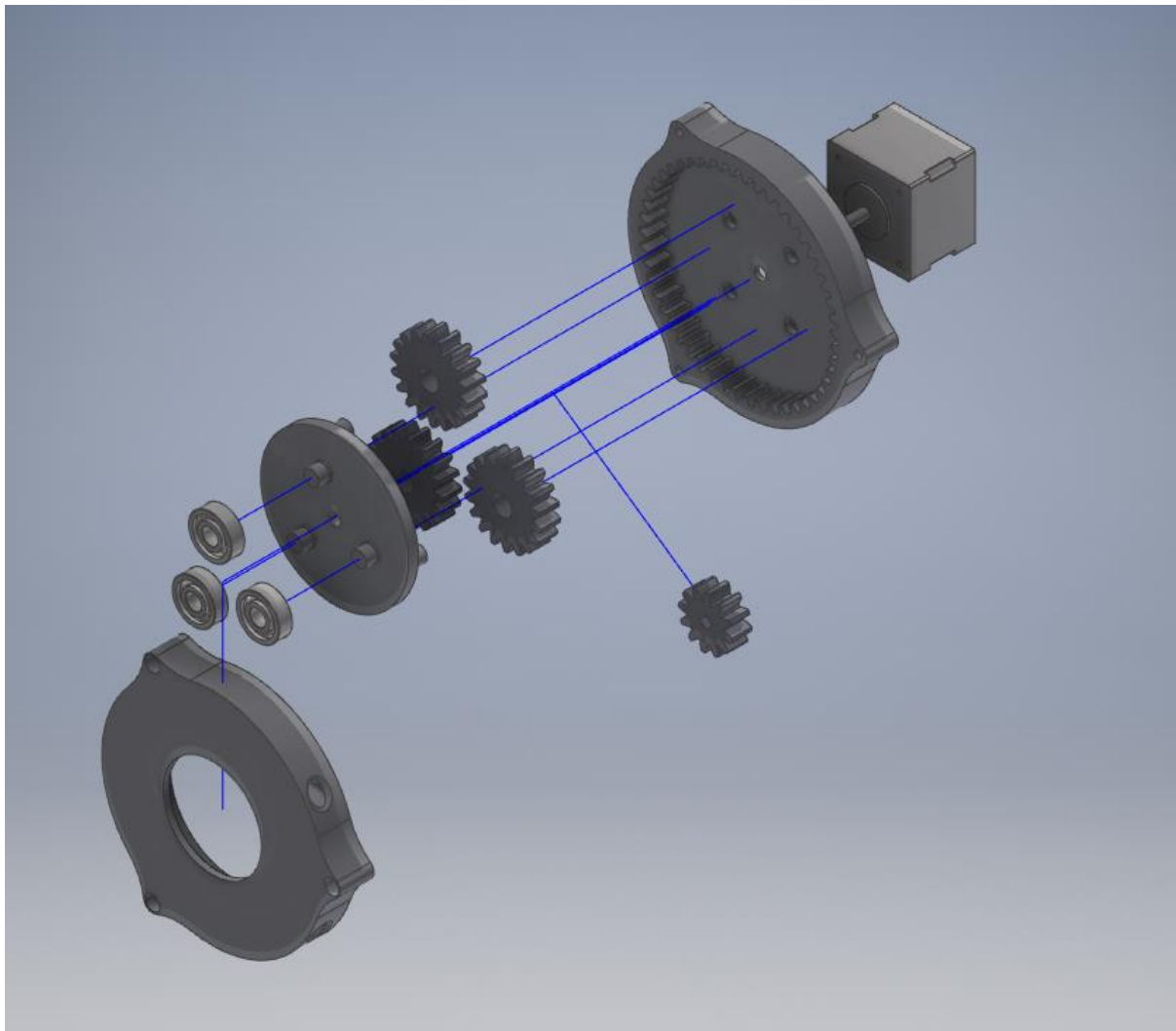


Figure 31 - redesigned peristaltic pump

Several design choices were carried over from the initial design, such as the diameter of the tubing, the choice of 608ZZ bearings, as well as the diameter of the arc along which the tube is compressed. The only major change consisted of the location of the entry and exit ports for the tubing into and out of the pump casing, which reduced the compression arc to  $180^\circ$  from  $270^\circ$ , further reducing the torque required to operate the pump.

## Pump calculations for redesigned pump

To achieve a printing speed of 100mm/s (0.1 m/s) with a 0.4mm nozzle:

Cross-sectional area of the nozzle:

$$A = \frac{\pi d^2}{4} = \frac{\pi (0.4 * 10^{-3})^2}{4} = 1.2566 * 10^{-7} m^2$$

With a flow velocity of 0.1 m/s, this corresponds to a volumetric flow rate of:

$$Q = Av = 1.2566 * 10^{-7} (0.1) = 1.2566 * 10^{-8} m^3/s$$

$$1.2566 * 10^{-8} * 1 * 10^6 = 0.0126 * 60 = 0.7539 ml/min$$

For a peristaltic pump:

$$Q \text{ in } \frac{ml}{minute} = \text{volume of occluded tubing} * \text{number of rollers} * \text{pump rpm}$$

The tubing has an ID of 3.5 mm, and is occluded along an arc of 271° with a radius of 32.5mm

Arc length

$$L = \frac{n}{360} * 2\pi r$$

$$L = \frac{180}{360} * 2 * \pi * 32.5 * 10^{-3} = 0.102m$$

Volume of the tubing

$$V = \frac{\pi d^2}{4} L = \frac{\pi * (3.5 * 10^{-3})^2}{4} 0.102 = 0.981 * 10^{-6} m^3 = 0.981 ml$$

Therefore, the pump must rotate at:

$$RPM = \frac{Q}{V * \text{no of rollers}} = \frac{0.7539}{* 3} = 0.256 RPM$$

Which is a very attainable speed, even for a motor reduced by a factor of 5.

## Theoretical steps per mm of “filament”

In order to know the correct length of filament to feed to the extruder, the 3D printer’s firmware knows the number of steps to send the motor in order to feed one mm of filament. In order to prepare the printer to use this pump, it is necessary to calculate the steps per mm for this pump.

As the ID of the tubing is given by the manufacturer as 3.5mm, the “filament” diameter can be assumed to be the same.

One revolution of the pump feeds  $0.981ml * 3 \text{ rollers} = 2.943ml$ .

$$\frac{4v}{\pi d^2} = L = \frac{4(2.943 * 10^{-6})}{\pi * (3.5 * 10^{-3})^2} = 0.306m \text{ of filament}$$

That means:

$$\frac{3200 \text{ steps}}{306mm} = 10.4575 \text{ steps per mm}$$

The completed pump is pictured below:

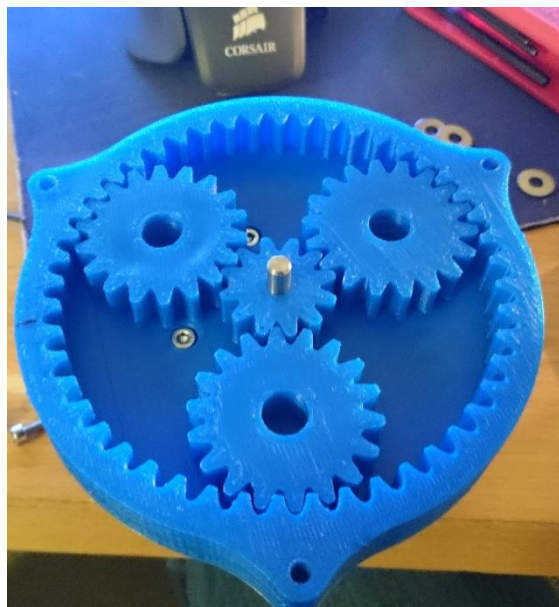


Figure 32 - Planetary gear mechanism, printed in blue PLA

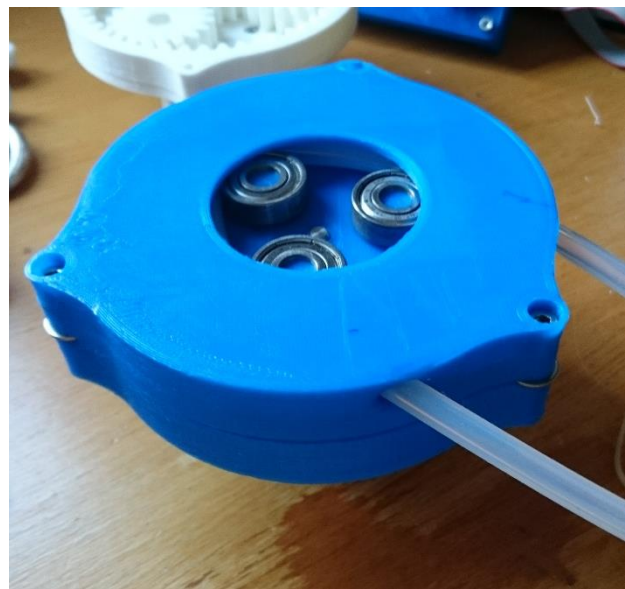


Figure 34 - Peristaltic pump, fully assembled



Figure 33 - Peristaltic pump with planet/bearing carrier installed

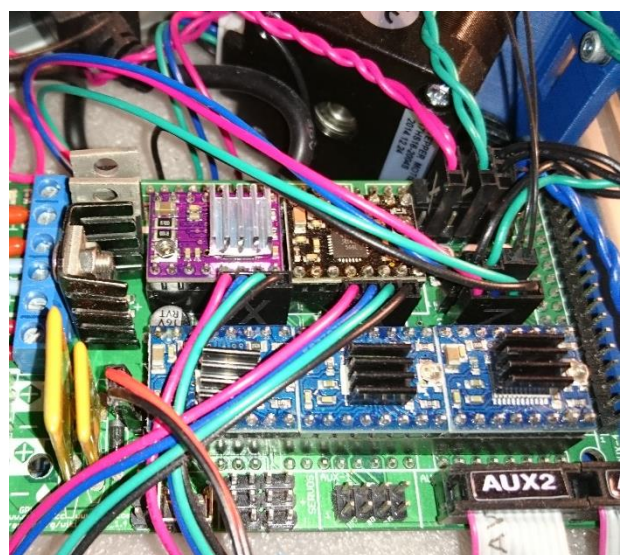


Figure 35 - upgraded DRV 8825 stepper driver (top left, purple PCB) installed on printer motherboard



Figure 36 - lid of peristaltic pump with tubing installed

## Installation of modified hot end

In order to prepare the 3D printer for conversion to PVC printing and to integrate the PVC feed system into the 3D printer, it was necessary to swap out the 3D printer's effector plate for a modified version. The hot end is secured to the effector plate using a locking clip which is then held in place by a set of 6xM3 bolts.



Figure 37 - modified effector plate

These bolts also secure a variety of other accessories to the 3d printer when the hot end is installed, such a supplemental cooling fan and a print bed levelling probe:



Figure 38 - effector plate installed in printer, and all electronics connected. note the hose barb visible in the center of the effector

Once the hot end was installed, the silicone tubing was connected to the peristaltic pump (see fig. 38). With all vital connections now made, it was possible to begin the first feed system test.

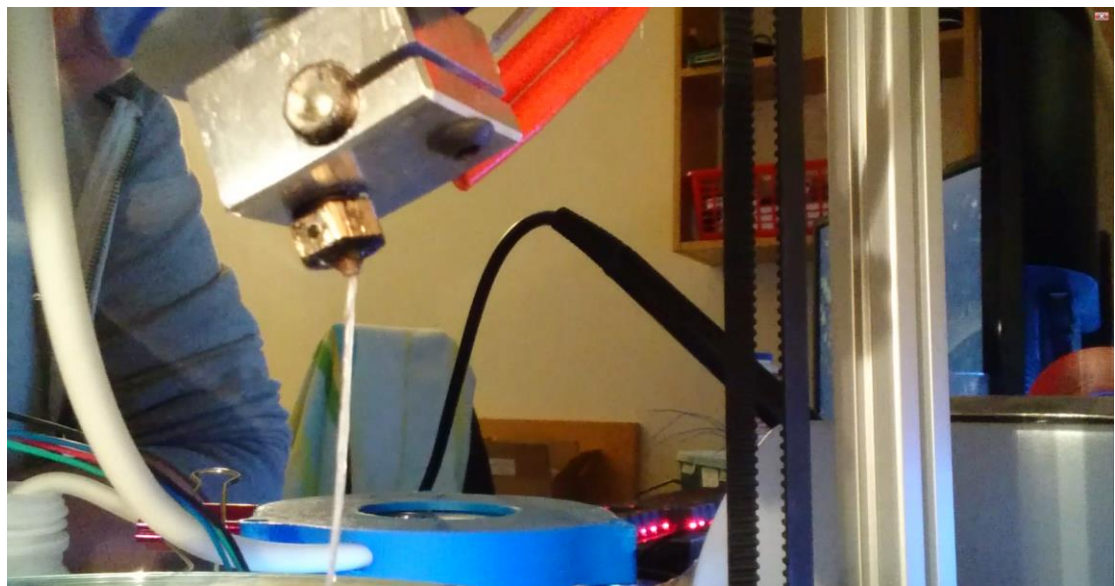


Figure 39 - extrusion test with peristaltic pump in background

### Discussion of first feed system test

The first feed system test with the redesigned pump went exactly as was originally hoped; the pump was able to produce sufficient pressure to extrude the PVC from the nozzle of the hot end, and the material cured sufficiently on its way through the hot zone. It was, however observed that the extruded filament of PVC was filled with bubbles, see below:



Figure 40 - extruded PVC showing air bubbles

As the PVC does not outgas or produce vapour at the temperatures experienced during the test (210°C-220°C) it was deduced that the bubbles originated from the raw solution. The PVC suspension tends to settle when stored for extended periods of time. In order to use the material, it must be gently shaken to restore a homogeneous mix to the suspension. As the suspension has a comparatively

high viscosity, the entrapped air (particularly very small bubbles) does not readily escape out of the solution.

Bubbling is an undesirable condition for 3D printing, as air in the extrusion path can cause localised weaknesses in the material which reduce the printed part's overall strength.

Additionally, it was observed that when the pump was made retract some pressure during printing (retractions are performed to prevent extruder "ooze"- the unintentional dragging of thin fibres of plastic behind the nozzle) the nozzle would temporarily lose pressure and would take too long to begin extruding material again. This condition is highly undesirable due to the fact that it causes underextrusion, a phenomenon caused by the deposition of too little plastic on the build surface. Underextrusion causes weak and porous prints which fail easily along the printing planes in the finished model.

Unfortunately, this condition proved very difficult to solve, as it was caused by backlash in the gearing. All gears require just enough space to clear the non-meshing teeth. This means that engaged teeth have a small amount of play – meaning that the two gears can move relative to each other without transferring the right amount of motion. This mechanical loss was aggravated by the fact that FDM 3D printers only possess limited precision - even the best 3D printed gears possess vastly more play than machined metal alternatives.

Finally, it was observed that, if left idle for too long at 210°C or higher, the nozzle of the printer would become clogged. On disassembly, it was found that the nozzle had clogged due to the PVC degrading inside the nozzle, causing a blackened plug to form in the extrusion path.



Figure 41 - degraded PVC plug

This occurrence of blockage highlights the importance of strict temperature control when attempting to print with PVC.

Corrective actions taken in response to results from feed system testing

Based on the information gathered during the initial round of feed system testing, three actions were taken, outlined below.

### 1. Nozzle clog problem

To solve this issue, both software and hardware solutions were implemented. Firstly, the printer nozzle was upgraded from a 0.4mm aperture brass nozzle to a 0.8mm stainless steel nozzle. Smaller nozzles, such as the 0.4mm nozzle being used cause higher backpressures in the feed system, and don't allow any "idle leakage" from the extruder – small amounts of plastic forced from the nozzle due to thermal expansion. This idle leakage reduces the build-up of overheated PVC in the nozzle.

Secondly, it is possible to reduce the amount of hot time by modifying the G-code so that the hot end only heats up immediately before beginning to print using the following line of G-code:

```
M109 S[first_layer_temperature]
```

Next, the printer can be told to deactivate the cartridge heater immediately after completing a print using the command:

```
M104 S0
```

In practice, these two changes have eliminated any further occurrences of nozzle clogging due to degraded PVC.

### 2. Replacement of the peristaltic pump

As it is not possible to produce the same pump design with no backlash, it was decided to replace the peristaltic pump entirely with a directly-driven (zero backlash) peristaltic pump.

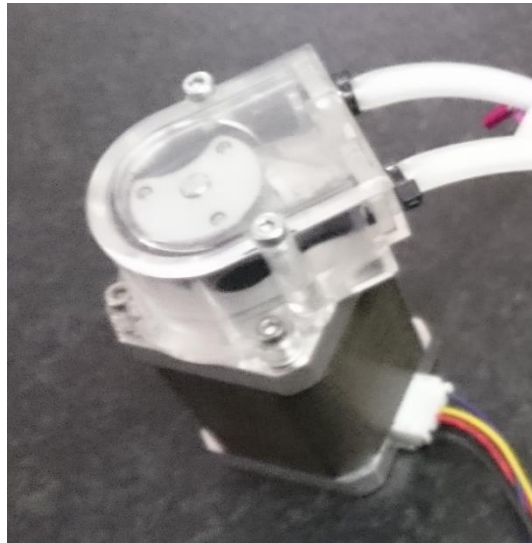


Figure 42 - purchased peristaltic pump

The purchased pump, with its direct-drive design, works perfectly when combined with the 65Ncm NEMA 17 motor, and has prevented any further occurrences of retraction/backlash-related underextrusion.

### 3. Bubble reduction / degassing

In order to address the bubble formation problem, it was decided to create a theoretical design for a degassing unit attached to the PVC reservoir. Before initiating a print, the reservoir would be reduced to about 0.5 Bar absolute pressure. This low vacuum would be maintained for one minute, after which the unit returns the reservoir to ambient pressure. To remove the maximum amount of bubbles from the PVC suspension, the system would pulse the vacuum, reducing the chamber pressure and returning to ambient repeatedly.

In practice, the PVC suspension was simply allowed to sit undisturbed for a minimum of one hour before initiating a print, giving the air plenty of time to bubble out.

### Calibration of new pump

The newly-bought pump had to be calibrated to allow the printer to use the extruder correctly. Unfortunately, exact data of tube diameters, etc. was not available from the manufacturer, so the steps/mm calibration had to be performed empirically.

To calibrate the pump through physical measurements, rather than by calculating the correct value, a way of controlling the motor had to be come up with. To this end, an Arduino mega 2560 was used in conjunction with a discarded Pololu A4988 stepper motor driver, in a configuration similar to the one pictured below:

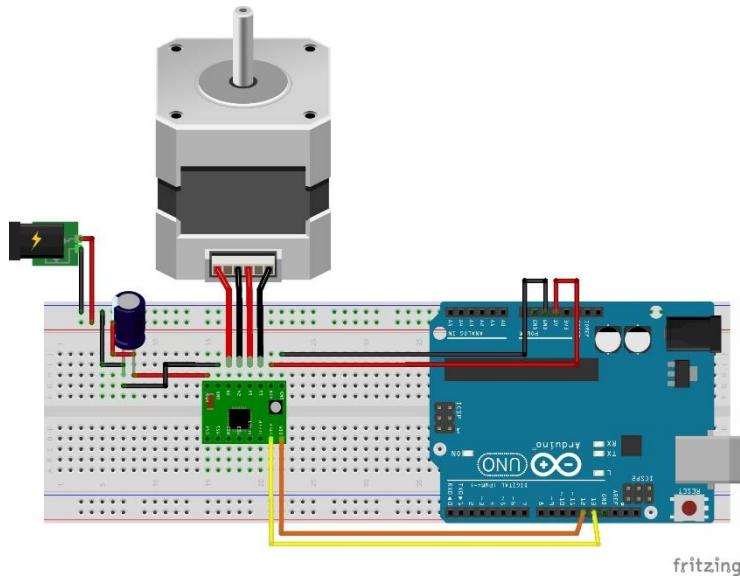


Figure 43 Pololu A4988 stepper motor driver connected to Arduino

For the 12V supply, a common mains-fed “power brick” was used, which provided power to both the Arduino (via the Vin pin) as well as the stepper driver through the Vmot pin.

Additionally, two buttons were added to send the motor 5000 steps in one direction or 5000 steps in the opposite direction.

The following Arduino Code was used:

```
#include<a4988.h> //A4988 stepper driver library

//define the which pins on the A4988 are connected to what
#define MS1PIN 8
#define MS2PIN 9
#define MS3PIN 10
#define DIRPIN 4
#define STEPPIN 5
#define ENABLEPIN 6
#define MOTOR_STEPS 200

//initiate an instance of the A4988 library object and call it "myA4988"
a4988 myA4988(MOTOR_STEPS, MS1PIN, MS2PIN, MS3PIN, DIRPIN, ENABLEPIN,
STEPPIN);

void setup() {
    //do not enable the motor on boot
    myA4988.enable(0);
    //set the stepper driver to 1/16th stepping mode
    myA4988.setStepMode(16);
    //sets the microsecond delay betweeen steps
    myA4988.setDelay(800);
}

void loop() {
    //if button A is pressed, send 5000 steps in one direction
    if(digitalRead(14) == HIGH) {
        myA4988.setDirection(0);
        myA4988.step(5000);
    }
    //if button B is pressed, send 5000 steps on the other direction
    if(digitalRead(15) == HIGH) {
        myA4988.setDirection(1);
        myA4988.step(5000);
    }
}
```

By filling the tube with water and running the pump, it was possible to measure the distance the water was moved through the tubing, making it possible to calculate back the number of steps per mm.

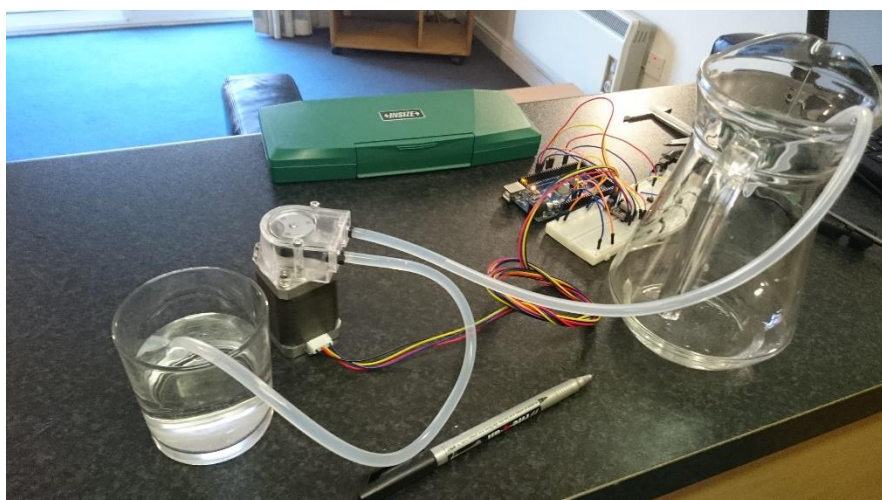


Figure 44 - simple water calibration setup

The meniscus of the water in the tube was marked off using a permanent marker. The pump was then set to run 5000 steps, and the displacement of the meniscus inside the tube was recorded. Ten runs were performed and an average value for steps per mm was calculated.

1/16th $\mu$ step calibration			
Run	Steps	distance	steps/mm
1	5000	64	78.1250
2	5000	64.06	78.0518
3	5000	64.46	77.5675
4	5000	64.12	77.9788
5	5000	64.6	77.3994
6	5000	63.98	78.1494
7	5000	64.63	77.3635
8	5000	63.94	78.1983
9	5000	63.81	78.3576
10	5000	64.13	77.9666
		avg	77.9158
		stdev	0.3304

The table shows a very close spread of measurement, indicating a very reliable measurement.

## PVC 3D printing

With these three main issues as well as pump calibration out of the way, it was possible to truly begin 3D printing with PVC, at first beginning with very simple shapes such as flat pucks with a 5cm diameter and 3mm thickness such as the one pictured below:



*Figure 45 - 3D printed PVC puck*

These pucks are well suited to detecting any telltale signs of 3D printing issues, such as gas inclusions, over or under extrusion or bad feed system calibration. Fortunately, the system worked extremely well with the aforementioned improvements, and it was possible to print a more complex demo piece: a scaled-down model of a human ear:



*Figure 46 - scaled-down model of a human ear, printed in soft PVC*

## Degassing system controller design

As a supplementary feature to the PVC 3D printer, an electronic vacuum chamber controller was designed. This controller, boasting USB connectivity and an on-board Atmega 328p microcontroller, was derived from the schematics of the Arduino Uno published on the Arduino website.

Among the included features are:

- Automatic voltage selection:
  - An LM358 Op-amp detects whether the system is run from the DC power jack or the built-in USB port, and chooses the correct power source.
- A FT232RL chip allows the Atmega 328p to communicate with a PC over USB
- USB serial traffic indicating LEDs – these LEDs flash when data is being transferred between the PC and the Arduino
- 12V power supply to power the vacuum pump
- DRV 8825 stepper motor carrier for the vacuum pump
- Arduino-compatible pin layout
- Hardware reset switch, as well as USB-reset functionality
- 10-pin programming header, providing a backup way to program the controller, should the USB connection fail
- MPX 2100AP absolute pressure sensor (feature pending)
  - The MPX 2100AP is an absolute pressure sensor with an operating range between atmospheric and absolute vacuum pressures, based on a silicon strain gauge/reference vacuum configuration

The system schematics are laid out in CADSoft EAGLE, a free schematic and PCB layout software.

The controller is designed to work with the discarded geared peristaltic pump. As peristaltic pumps have positive displacement, they are also capable of producing a fairly strong vacuum.

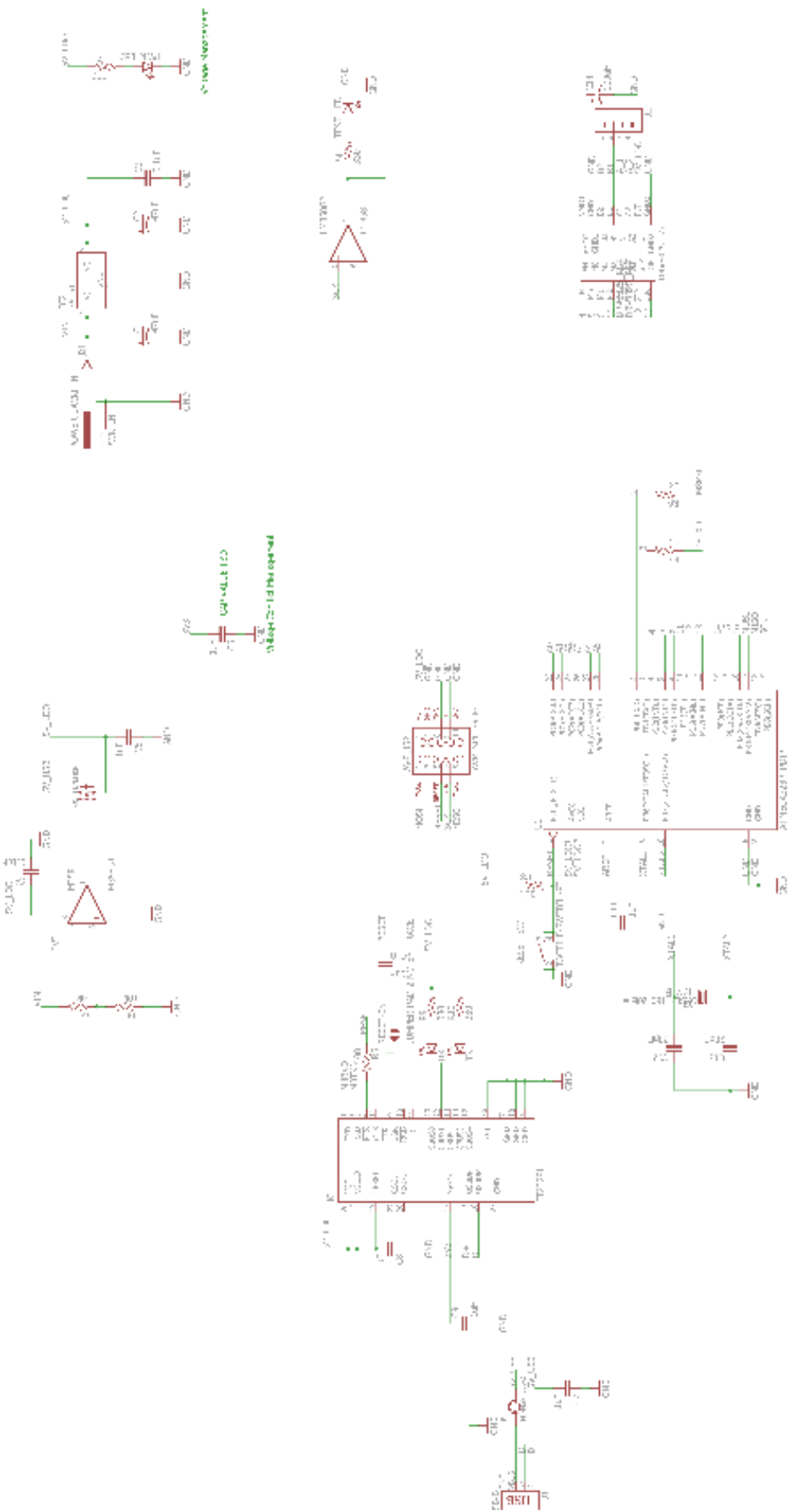


Figure 47 - Schematic of Arduino-based vacuum controller

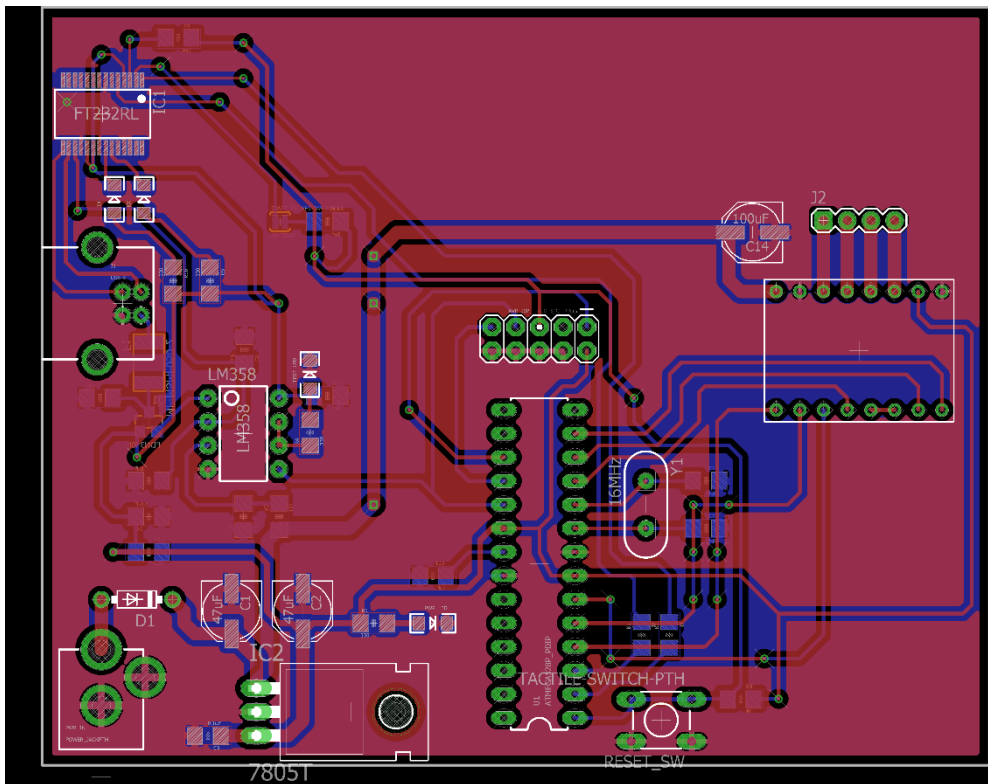


Figure 48 - Vacuum pump controller PCB

## Comparison of 3D printed PVC with conventionally manufactured PVC

The final of the initial three goals of the project was to compare the PVC produced by the 3D printer with PVC that had been conventionally manufactured, i.e. cast PVC.

Due to time and equipment constraints in CIT, it was only possible to perform a tensile test as a comparative metric, as there are no Shore hardness testers in the college.

ISO 37:2011 – Rubber, vulcanised or thermoplastic – determination of tensile stress-strain properties

ISO 37 describes methods for testing the tensile properties of elastomers by destructive testing in a tensile testing machine. It provides two main methods of testing: using ring test pieces or dumbbell test pieces. Due to the comparative ease with which dumbbell test pieces can be manufactured, it was decided to use the latter.

### Dumbbell test pieces

The standard prescribes four different sizes of dumbbell for use in different scenarios, however due to the limited quantity of PVC on hand, type 4 dumbbell geometry was selected.

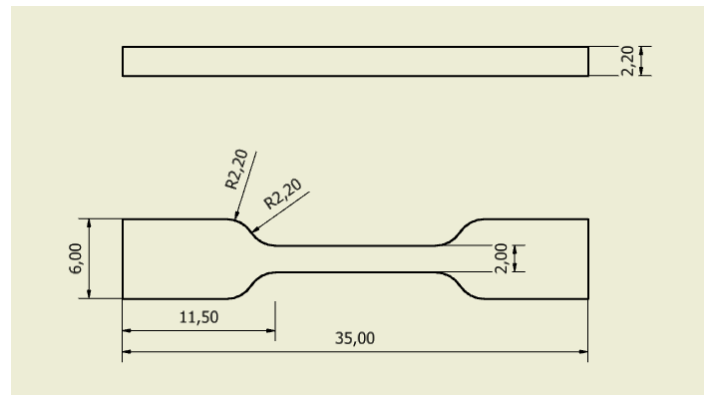


Figure 49 - ISO 37 type 4 dumbbell. All dimensions in mm.

To manufacture the cast test pieces, a mould was built from a spare piece of aluminium stock using the CNC milling centres in CIT. A solid model of the mould was transferred to a workshop computer running AlphaCAM. A toolpath was created to mill out the exact geometry required, and a piece was produced (pictured below).

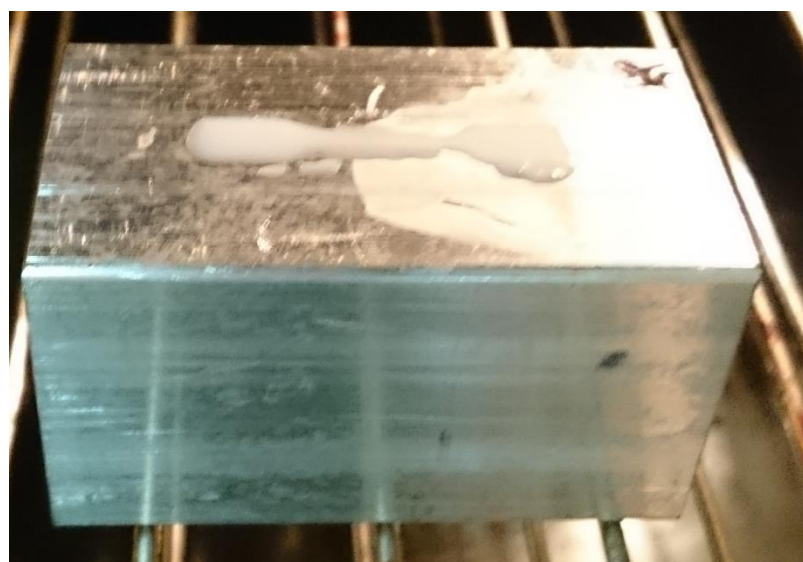


Figure 50 - mould for production of cast test pieces

The moulds were filled with PVC using a syringe to dispense the right quantity of PVC, and then placed in the oven at 250°C where the PVC was allowed to cure until glassy, a colour change which indicates that the right curing state of the PVC has been reached.



*Figure 51 - filling a mould with PVC*



*Figure 52 - Dumbbell mould in the oven to cure*

At the same time, the PVC 3D printer produced five samples of 3D printed PVC dumbbells of the same geometry, also printed at 250°C, in order to obtain a one-for-one comparison.

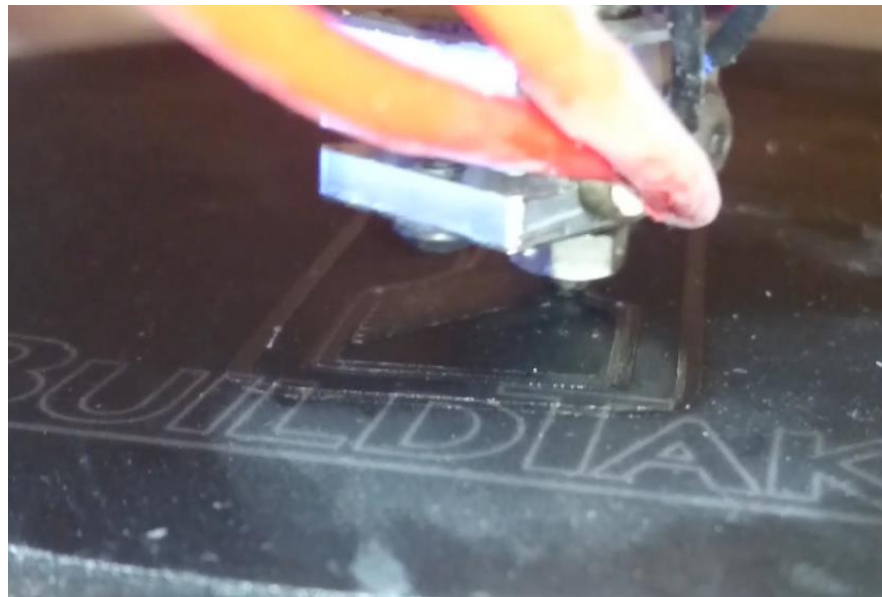


Figure 53 - 3D printer producing a PVC object

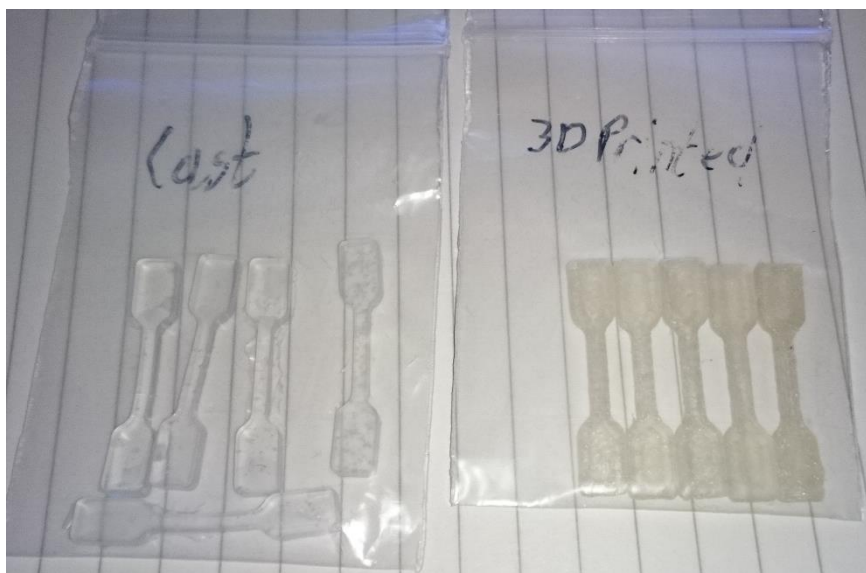


Figure 54 - Cast and 3D printed tensile testing samples side-by-side

## Tensile testing

The testing was carried out on the Instron tensile testing machine in the Mechanics laboratory in the A block of CIT. Testing was unfortunately not carried out under temperature-controlled conditions as described in ISO 37, however as the samples were stored together for over a week it is not expected that environmental factors played a large role in the results. It should be noted that it is only possible to compare the tensile properties of the 3D printed PVC parallel to the grain, as it is not possible to print such a thin and soft structure without being encased in support material.

### Procedure

The machine was set up with a gauge length of 10mm and a strain rate of 100mm per minute. Samples were tightly clamped in the jaws of the machine in order to prevent sample slippage. Care was taken to ensure samples were correctly aligned in the machine, as pictured below:

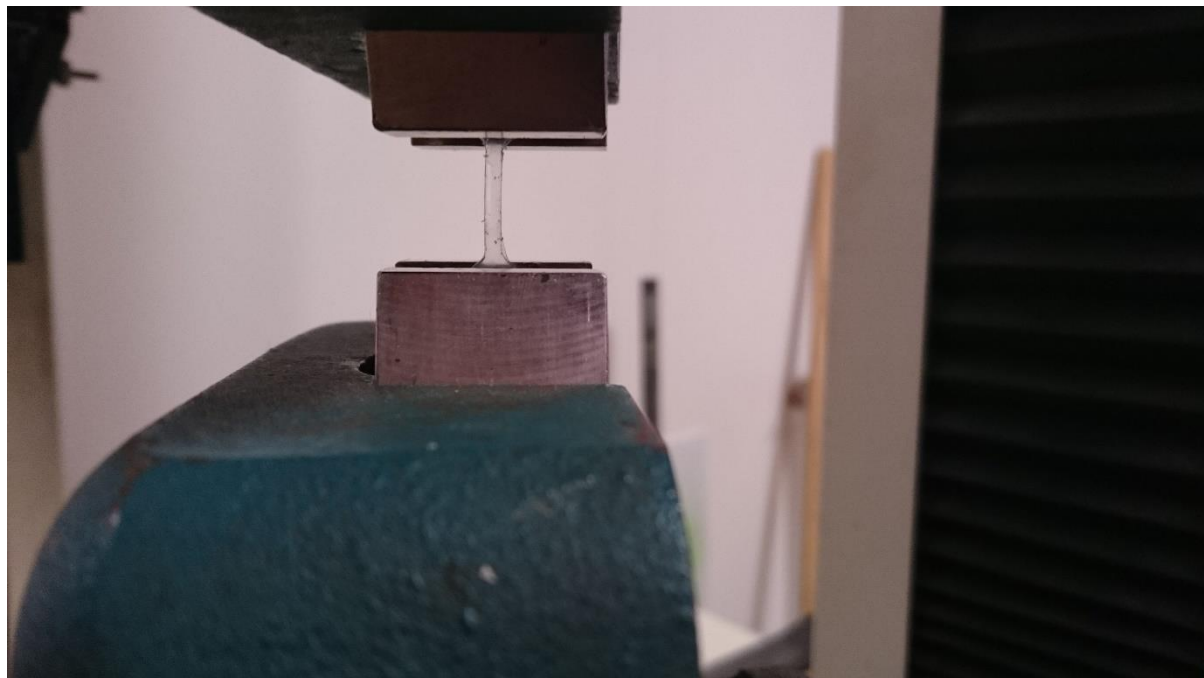


Figure 55 - cast test piece in tensile tester jaws

Once the sample was firmly secured, the test was initiated.

## Tensile testing results, 3D printed

	Ultimate tensile strength (MPa)	Tensile strength at break (MPa)	Elongation at break (%)
Specimen 1	4.3545	4.2955	600%
Specimen 2	2.8886	2.8409	283%
Specimen 3	4.3727	4.3273	599%
Specimen 4	4.3091	4.1682	564%
Specimen 5	4.7909	4.7341	672%
Average value	4.1432	4.0732	544%
Standard deviation	0.6509	0.6447	1.3487

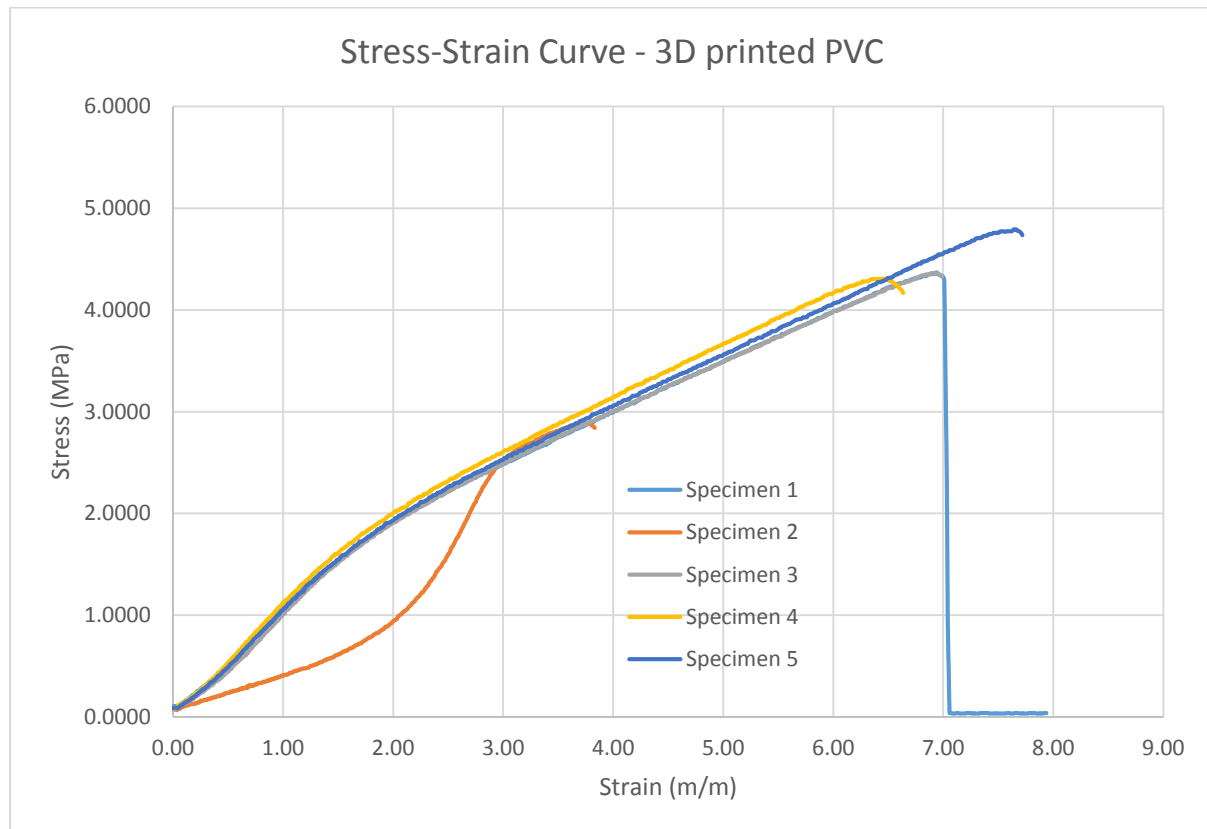


Figure 56 - Stress-Strain curve, 3D printed PVC

## Tensile testing results, Cast

	Ultimate tensile strength (MPa)	Tensile strength at break (MPa)	Elongation at break (%)
Specimen 1	3.7500	3.6955	464%
Specimen 2	1.4841	1.4705	109%
Specimen 3	2.8182	2.8091	372%
Specimen 4	4.0455	3.9909	602%
Specimen 5	2.4000	2.3864	386%
Average value	2.8995	2.8705	387%
Standard deviation	0.9269	0.9093	1.6104

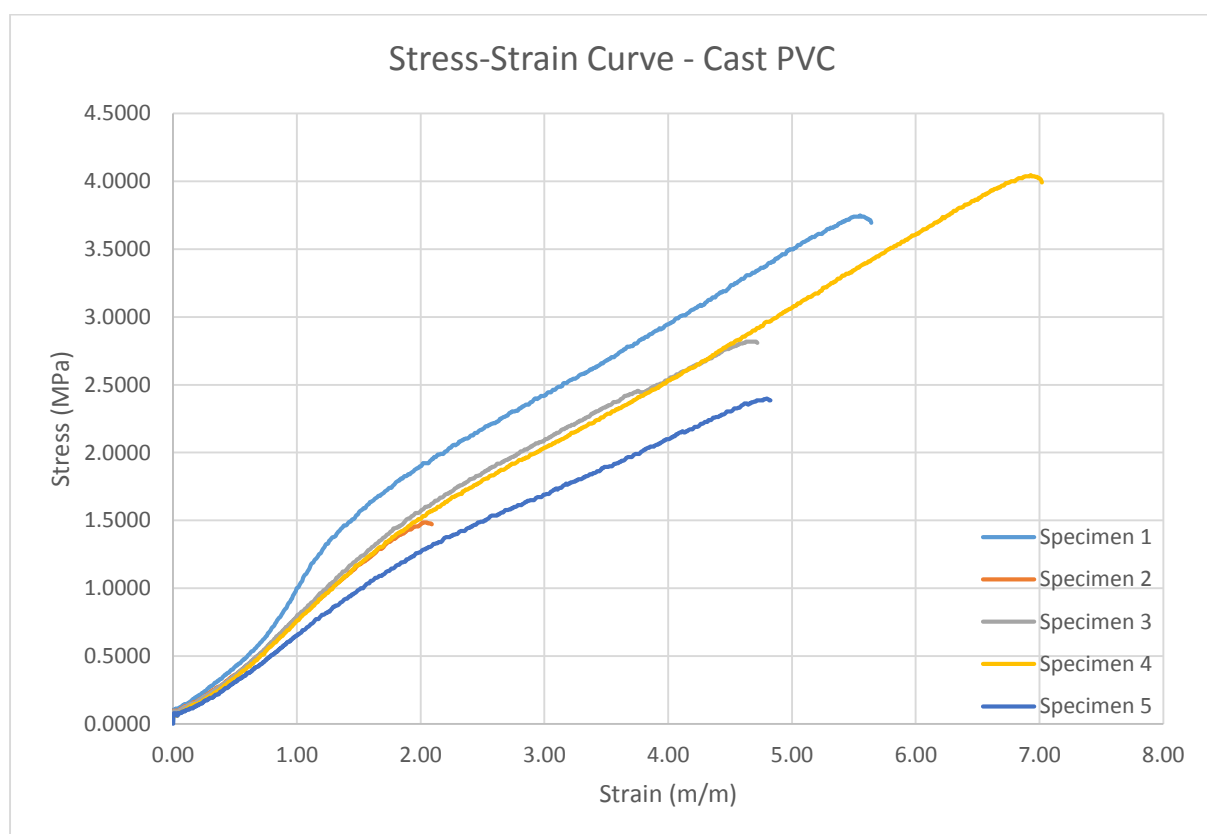


Figure 57 - Stress-Strain Curve, Cast PVC

### Discussion of tensile testing results

Contrary to expectation, the 3D printed PVC proved to be about 43% stronger, both in ultimate tensile strength and in tensile strength at break. However, these results should be regarded with caution; firstly, these are very small sample sizes for an effective and statistically significant comparison, and secondly, the results contain some distorting factors. When the cast dumbbells were made, they were cast without a degassing step. This led to some of the samples being filled with bubbles and cavities, which negatively impact the mechanical properties of the samples. Furthermore, problems were encountered when clamping the samples in the tensile tester, as some samples slipped out from between the jaws of the clamp and had to be retested, which may damage the sample prior to retesting. Specimen 2 for example was strained almost to breaking, but slipped from the chuck of the machine. Retesting the sample gave a very low UTS and breaking strength when compared with the other samples.

All in all, these results are an interesting indicator, showing the possibility that the 3D printed PVC may actually have a significantly higher tensile strength than cast PVC

### Conclusion

Originally, this project was intended to achieve three major goals; The first goal, to examine the possibility of additive manufacturing with soft PVC was achieved in October of 2015 with the initial feasibility testing showing that PVC can be extruded through a common hot-end at pressures attainable by a 3D printer. The second goal, to integrate the feed system into a 3D printer and actually print with it was reached in late April with the production of a model of a human ear as well as a collection of test pieces to diagnose extrusion problems and material properties. Finally, the last goal has also been reached, if not quite conquered; it would have been much better to have had the time to produce and test large sample sizes to acquire statistically significant data, as well as being able to compare other material properties, particularly shore hardness.

Finally, I can say I regard this project as being enormously successful for myself; not only was the original idea proven to work, but I was able to access a wealth of knowledge in fields range from electronic design and mechanical design, to material science, chemistry, control theory, biology, CAD/CAM and biomedical manufacturing.

## References

1. PVC medical devices | PVCMed.org [WWW Document], n.d. URL <http://pvcmed.org/pvc-in-healthcare/pvc-medical-devices/> (accessed 5.12.16).
2. PVC for Health - PVC [WWW Document], n.d. URL <http://www.pvc.org/en/p/health> (accessed 5.12.16).
3. Krähling, H., 1999. Life cycle assessments of PVC products: green guides to ecological sustainability, LCA documents. Eco-Informa-Press, Bayreuth.
4. Baumann, E. (1872) "Über einige Vinylverbindungen" (On some vinyl compounds), Annalen der Chemie und Pharmacie, 163 pgs. 315-318.
5. Zhao, Xiaobin and Courtney, James M. (2009) "Update on Medical Plasticised PVC", Smithers Rapra, pg. 9
6. Somkuti, S.G., Tilson, H.A., Brown, H.R., Campbell, G.A., Lapadula, D.M., Abou-Donia, M.B., 1988. Lack of Delayed Neurotoxic Effect after Tri-o-cresyl Phosphate Treatment in Male Fischer 344 Rats: Biochemical, Neurobehavioral and Neuropathological Studies. *Toxicol. Sci.* 10, 199–205. doi:10.1093/toxsci/10.2.199
7. <http://www2.deloitte.com/content/dam/Deloitte/global/Documents/Technology-Media-Telecommunications/gx-tmt-pred15-3d-printing-revolution.pdf>
8. [What is 3D printing? How does 3D printing work? \[WWW Document\], n.d. URL http://3dprinting.com/what-is-3d-printing/#processesandtechnologies \(accessed 5.12.16\).](http://3dprinting.com/what-is-3d-printing/#processesandtechnologies)
9. Rubber-Like Materials for 3D Printing | Stratasys [WWW Document], n.d. URL <http://www.stratasys.com/materials/polyjet/rubber-like> (accessed 5.12.16).
10. Crump, S.S., 1992. Apparatus and method for creating three-dimensional objects. US5121329 A.
11. Wohlers Associates [WWW Document], n.d. URL <http://wohlersassociates.com/2013report.htm> (accessed 5.12.16).
12. Team, P.I., others, 2014. 3D Printing. Intellectual Property Office, 3D Printing (May 29, 2014). Intellectual Property Office Research Paper.
13. Home [WWW Document], n.d. . Creative Commons. URL <https://creativecommons.org/> (accessed 5.12.16).
14. Industry, S. of the P., Berins, M.L., 1991. SPI plastics engineering handbook of the Society of the Plastics Industry, Inc. Van Nostrand Reinhold.

15. PHTHALATE PLASTICIZERS [WWW Document], n.d. URL  
[http://wwwcourses.sens.buffalo.edu/ce435/2001ZGu/Phthalate\\_Plasticizers/PhthalatePlasticizersReport.htm](http://wwwcourses.sens.buffalo.edu/ce435/2001ZGu/Phthalate_Plasticizers/PhthalatePlasticizersReport.htm) (accessed 5.3.16).
16. Immergut, E.H., Mark, H.F., 1965. Principles of Plasticization, in: Platzer, N.A.J. (Ed.), Plasticization and Plasticizer Processes. AMERICAN CHEMICAL SOCIETY, WASHINGTON, D.C., pp. 1–26.
17. Plasticisers [WWW Document], n.d. . Plasticisers. URL  
[http://www.plasticisers.org/en\\_GB/plasticisers](http://www.plasticisers.org/en_GB/plasticisers) (accessed 5.3.16).
18. [https://echa.europa.eu/documents/10162/13641/dehp\\_echa\\_review\\_report\\_2010\\_6\\_en.pdf](https://echa.europa.eu/documents/10162/13641/dehp_echa_review_report_2010_6_en.pdf)
19. Caldwell, J.C., 2012. DEHP: Genotoxicity and potential carcinogenic mechanisms—A review. Mutation Research/Reviews in Mutation Research 751, 82–157.  
doi:10.1016/j.mrrev.2012.03.001
20. Li, M., Qiu, L., Zhang, Y., Hua, Y., Tu, S., He, Y., Wen, S., Wang, Q., Wei, G., 2013. Dose-related effect by maternal exposure to di-(2-ethylhexyl) phthalate plasticizer on inducing hypospadiac male rats. Environmental Toxicology and Pharmacology 35, 55–60.  
doi:10.1016/j.etap.2012.10.006
21. Wang, Y.-X., You, L., Zeng, Q., Sun, Y., Huang, Y.-H., Wang, C., Wang, P., Cao, W.-C., Yang, P., Li, Y.-F., Lu, W.-Q., 2015. Phthalate exposure and human semen quality: Results from an infertility clinic in China. Environmental Research 142, 1–9.  
doi:10.1016/j.envres.2015.06.010
22. Eckert, E., Münch, F., Göen, T., Purbojo, A., Müller, J., Cesnjevar, R., 2016. Comparative study on the migration of di-2-ethylhexyl phthalate (DEHP) and tri-2-ethylhexyl trimellitate (TOTM) into blood from PVC tubing material of a heart-lung machine. Chemosphere 145, 10–16.  
doi:10.1016/j.chemosphere.2015.11.067
23. Marcilla, A., Garcia, S., Garcia-Quesada, J.C., 2008. Migrability of PVC plasticizers. Polymer Testing 27, 221–233. doi:10.1016/j.polymertesting.2007.10.007
24. Epicyclic Gears [WWW Document], n.d. URL  
[http://www.roymech.co.uk/Useful\\_Tables/Drive/Epi\\_cyclic\\_gears.html](http://www.roymech.co.uk/Useful_Tables/Drive/Epi_cyclic_gears.html) (accessed 5.13.16).